THESIS APPROVAL

GRADUATE SCHOOL, KASETSART UNIVERSITY

Master of Science (Chemistry)
DEGREE

Chemistry
FIELD

Chemistry
DEPARTMENT

TITLE: Experimental and Theoretical Studies of 9-octyl-3,6-di(thiophen-2-yl)-Carbazole Derivatives

NAME: Ms. Suwannee Sriyab

THIS THESIS HAS BEEN ACCEPTED BY

THESIS ADVISOR
(Mr. Songwut Suramitr, Ph.D.)

THESIS CO-ADVISOR
(Associate Professor Supa Hannongbua, Dr.rer.nat.)

THESIS CO-ADVISOR
(Mr. Jakkapan Sirijareansre, Ph.D.)

DEPARTMENT HEAD
(Associate Professor Supa Hannongbua, Dr.rer.nat.)

APPROVED BY THE GRADUATE SCHOOL ON

DEAN
(Associate Professor Gunjana Theeragool, D.Agr.)

THESIS

EXPERIMENTAL AND THEORETICAL STUDIES OF 9-OCTYL-3,6-DI(THIOPHEN-2-YL)-CARBAZOLE DERIVATIVES

SUWANNEE SRIYAB

A Thesis Submitted in Partial Fulfillment of
the Requirements for the Degree of
Master of Science (Chemistry)
Graduate School, Kasetsart University
2011

Suwannee Sriyab 2011: Experimental and Theoretical Studies of 9-octyl-3,6-di(thiophen-2-yl)-Carbazole Derivatives. Master of Science (Chemistry), Major Field: Chemistry, Department of Chemistry. Thesis Advisor: Mr. Songwut Suramitr, Ph.D. 78 pages.

The molecular structural and electronic properties of 9-octyl-3,6-di(thiophen-2-yl)-Carbazole and its derivatives were studied by quantum chemical calculations. Methyl (CH_3), formyl (CHO) and acetyl ($COCH_3$) substitutions have been applied on 9-octyl-3,6-di(thiophen-2-yl)-Carbazole to investigate the optical properties. All structures were optimized using PBE0 functional of calculations with the 6-31G(d) basis set. The electronic transition of structural geometries have been studied by PCM-TD-PBE0/6-311G(d,p) calculations based on ground state geometries at PBE0/6-31G(d) level. The obtained results indicate that calculated UV-vis absorption spectra of Th-3,6CZ-Th-H, Th-3,6CZ-Th-CH_3, Th-3,6CZ-Th-$COCH_3$ and Th-3,6CZ-Th-CHO were found at 298, 334, 393 and 402 nm with respect to the experimental data of 302, 298, 365 and 393 nm, respectively. The fluorescence quantum yield and fluorescence lifetimes of the compound in dichloromethane has been studied. The results showed Th-3,6CZ-Th-$COCH_3$ and Th-3,6CZ-Th-CHO had high quantum yield. Most of the derivative of Th-3,6CZ-Th-H molecule exhibit planar structures at excitation state. The excited state-torsion angles are more planar than the ground state geometries. The obtained results of the electronic transition of structural geometries indicate that calculated absorption and emission spectra related with the experimental data. In additional, the polarizable continuum model was successfully applied to include solvent effect in the model which plays an important role on the absorption behavior.

Student's signature

Thesis Advisor's signature

___ / ___ / ___

ACKNOWLEDGEMENTS

I sincerely thank my advisor, Dr. Songwut Suramitr for his advice, suggestion, tremendous support and meticulous attention throughout the duration of my graduate study and research. I am particularly grateful to my advisory committee Associate Professor Dr. Supa Hannongbua and Dr. Jakkapan Sirijareansre, the representative of Graduate School, for their worthy suggestion and constructive criticism.

Financial supports were from the Thailand Research Fund (TRF), Ministry of Education through the “National Research University Project of Thailand (NRU)” and the “National Center of Excellence for Petroleum, Petrochemical and Advanced Materials (NCE-PPAM). My colleagues at Laboratory for Computational and Applied Chemistry (LCAC) are sincere thanked for their providing helpful assistance and sharing useful ideas and I would also like to thank all of staffs at Department of Chemistry, Faculty of Science, Kasetsart University for research facilities.

Finally, I am especially appreciated my parents, friends and colleagues at LCAC for their encouragement, sincere care and support throughout my entire study.

Suwannee Sriyab
April 2011

TABLE OF CONTENTS

Page

TABLE OF CONTENTS i
LIST OF TABLES ii
LIST OF FIGURES iii
LIST OF ABBREVIATIONS vi
INTRODUCTION 1
OBJECTIVES 6
LITERATURE REVIEW 7
MATERIALS AND METHODS 11
RESULTS AND DISCUSSION 23
CONCLUSION AND RECOMMENDATION 53
    Conclusion 53
    Recommendation 54
LITERATURE CITED 55
APPENDICES 62
    Appendix A Supporting information 63
    Appendix B Presentation and proceeding 71
CURRICULUM VITAE 78

LIST OF TABLES

Table **Page**

1 Optical data of Th-3,6Cz-Th-H, Th-3,6Cz-Th-CH_3, Th-3,6Cz-Th-$COCH_3$, and Th-3,6Cz-Th-CHO measured in dichloro-methane solution. 28

2 Optimized bond lengths (in Å) of Th-3,6Cz-Th-R (R = H, CH_3, $COCH_3$ and CHO) obtained from PBE0/6-31G(d) and PCM-TD-PBE0/6-311G(d,p) methods. 33

3 Optimized torsion angle (in degree) of Th-3,6Cz-Th-R (R = H, CH_3, $COCH_3$ and CHO) obtained from PBE0/6-31G(d) and PCM-TD-PBE0/6-311G (d,p) methods. 40

4 The lowest excitation energies in eV and oscillator strength (*f*) in solvent phase (in dichloromethane) using TD-PBE0/6-311G(d,p) method and absorption of experimental data in CH_2Cl_2 solution for the Th-3,6Cz-Th-R (R = H, CH_3, $COCH_3$ and CHO) geometries. H denoted HOMO and L is LUMO. 42

5 The emission energies in eV and oscillator strength (*f*) in solvent phase (in dichloromethane) using TD-PBE0/6-311G(d,p) method and emission of experimental data in CH_2Cl_2 solution for the Th-3,6Cz-Th-R (R = H, CH_3, $COCH_3$ and CHO) geometries. H denoted HOMO and L is LUMO. 51

6 The wavelength of emission energies, stokes shifts and radiative lifetime (τ) using TD-PBE0/6-311G(d,p) method and experimental data in CH_2Cl_2 solution for the Th-3,6Cz-Th-H, Th-3,6Cz-Th-CH_3, Th-3,6Cz-Th-$COCH_3$, and Th-3,6Cz-Th-CHO. 52

LIST OF FIGURES

Figure		Page
1	Organic Light Emitting Diode Diagram.	2
2	Process of organic light-emitting diodes (OLED).	3
3	Synthesis of 9-octyl-3,6-di(thiophen-2-yl)-carbazole derivatives. (R = -CH_3, -$COCH_3$ and -CHO)	12
4	Schematic diagram of (a) Th-3,6Cz-Th-H and (b) Th-3,6Cz-Th-CH_3 structures.	20
5	Schematic diagram of (a) Th-3,6Cz-Th-CHO and (b) Th-3,6Cz-Th-$COCH_3$ structures.	21
6	Absorption spectra of Th-3,6Cz-Th-H, Th-3,6Cz-Th-CH_3, Th-3,6Cz-Th-$COCH_3$ and Th-3,6Cz-Th-CHO in CH_2Cl_2 solution.	27
7	Emission spectra of Th-3,6Cz-Th-H, Th-3,6Cz-Th-CH_3, Th-3,6Cz-Th-$COCH_3$ and Th-3,6Cz-Th-CHO measured in dichloromethane solution.	29
8	Schematic represent the bond number on backbone structure of Th-3,6Cz-Th-R molecule.	32
9	Optimized bond length and bond length alternation (BLA) of Th-3,6Cz-Th-H of the S_0 and S_1 geometries as obtained from PBE0/6-31G(d) and TD-PBE0/6-311G(d,p) methods, respectively.	35
10	Optimized bond length and bond length alternation (BLA) of Th-3,6Cz-Th-CH_3 of the S_0 and S_1 geometries as obtained from PBE0/6-31G(d) and TD-PBE0/6-311G(d,p) methods, respectively.	36
11	Optimized bond length and bond length alternation (BLA) of Th-3,6Cz-Th -$COCH_3$ of the S_0 and S_1 geometries as obtained from PBE0/6-31G(d) and TD-PBE0/6-311G(d,p) methods, respectively.	37

LIST OF FIGURES (Continued)

Figure **Page**

12 Optimized bond length and bond length alternation (BLA) of Th-3,6Cz-Th -CHO of the S_0 and S_1 geometries as obtained from PBE0/6-31G(d) and TD-PBE0/6-311G(d,p) methods, respectively. 38

13 Schematic represent the bond number of Th-3,6Cz-Th-R (R = H, CH_3, $COCH_3$ and CHO) molecule. 39

14 Absorption spectra of Th-3,6Cz-Th-H obtained from the experimental in CH_2Cl_2 solution and calculated using TD-PBE0/6-311G(d,p) in PCM model. 45

15 Absorption spectra of Th-3,6Cz-Th-CH_3 obtained from the experimental in CH_2Cl_2 solution and calculated using TD-PBE0/6-311G(d,p) in PCM model. 46

16 Absorption spectra of Th-3,6Cz-Th-$COCH_3$ obtained from experimental in CH_2Cl_2 solution and calculated using TD-PBE0/6-311G(d,p) in PCM model. 47

17 Absorption spectra of Th-3,6Cz-Th-CHO obtained from the experimental in CH_2Cl_2 solution and calculated using TD-PBE0/6-311G(d,p) in PCM model. 48

18 Structures of molecular orbitals for (a) Th-3,6Cz-Th-H, (b) Th-3,6Cz-Th-CH_3, (c) Th-3,6Cz-Th-$COCH_3$ and (d) Th-3,6Cz-Th-CHO molecules. 50

LIST OF FIGURES (Continued)

Appendix Figure **Page**

A1 ^{1}H-NMR spectrum of 3,6-dibromo-9H-carbazole. 64

A2 ^{1}H-NMR spectrum of 3,6-Dibromo-9-octyl-carbazole. 65

A3 ^{1}H-NMR spectrum of 9-octyl-3,6-di(thiophen-2-yl)-carbazole. 66

A4 ^{1}H-NMR spectrum of 5,5’-(9-octyl-carbazole-3,6-diyl)-dithiophene-2-carbaldehyde. 67

A5 ^{1}H-NMR spectrum of 1,1’-(5,5’-(9-octyl-carbazole-3,6-diyl)-bis-(thiophene-5,2-diyl))-diethanone. 68

LIST OF ABBREVIATIONS

Abs. = Absorbance

Å = Aungstrom

°c = Degree celsius

CH_2Cl_2 = Dichloromethane

$CHCl_3$ = Chloroform

DFT = Density Functional Theory

g = Gram

^{1}H-NMR = Proton Nuclear Magnetic Resonance

HOMO = Highest Occupied Molecular Orbital

LUMO = Lowest Unoccupied Molecular Orbital

MHz = Megahertz

mmol = Millimolar

mL = Milliliter

nm = Nanometer

OLED = Organic Light Emitting Diode

PCM = Polarizable Continuum Model

S_0 = Ground state

S_1 = First singlet excited state

TD-DFT = Time-Dependent Density Function Theory

EXPERIMENTAL AND THEORETICAL STUDIES OF 9-OCTYL-3,6-DI(THIOPHEN-2-YL)-CARBAZOLE DERIVATIVES

INTRODUCTION

In 1987, the thin multilayer organic light emitting diodes (OLEDs) was recognized as one of the potential technologies for the next generation of flat-panel display device. The OLED composed of two layers of a hole-transporting layer and emitting material which are sandwich between an indium-tin-oxide anode and an alloyed Mg:Ag (Van Slyke, 1987). Electron-hole recombination is emitted as green electroluminescent. After that, the performances of OLED devices have been extensively improved such as turn-on voltage (Cao *et al*., 1999), external efficiency (Malinsky *et al*., 1999), current density (Cleave *et al*., 1999) and luminescence (Ogundare *et al*., 2008). The OLED component is composed of a cathode, an emissive layer, a conductive layer, an anode and a substrate (Figure 1). One of the simplest OLED is consisted of indium tin oxide (ITO) anode (Doskocz *et al*., 2006), hole-transporting layer (HTL), electron-transporting layer (ETL), and Mg-Ag cathode, in which HTL or/and ETL could act as the light-emitting layer (Tang *et al*., 1987; Fong *et al*., 2006; Tong *et al*., 2007). The ITO anode is a transparent semiconductor, which was used for the hole injection due to its work function of 4-5 eV (Paliulis *et al*., 2003). During last decade, the intensive research has been carried out to generate the material with high light emitting efficiencies (Shirota *et al*., 1994), high thermal stability, and good amorphous film formation property (Shirota *et al*., 2000). The electro-luminescence (EL) characteristic of OLED materials depend on the appropriate HOMO and LUMO energy levels and the electron and hole motilities (Pan *et al*., 2005; Brunner *et al*., 2004).

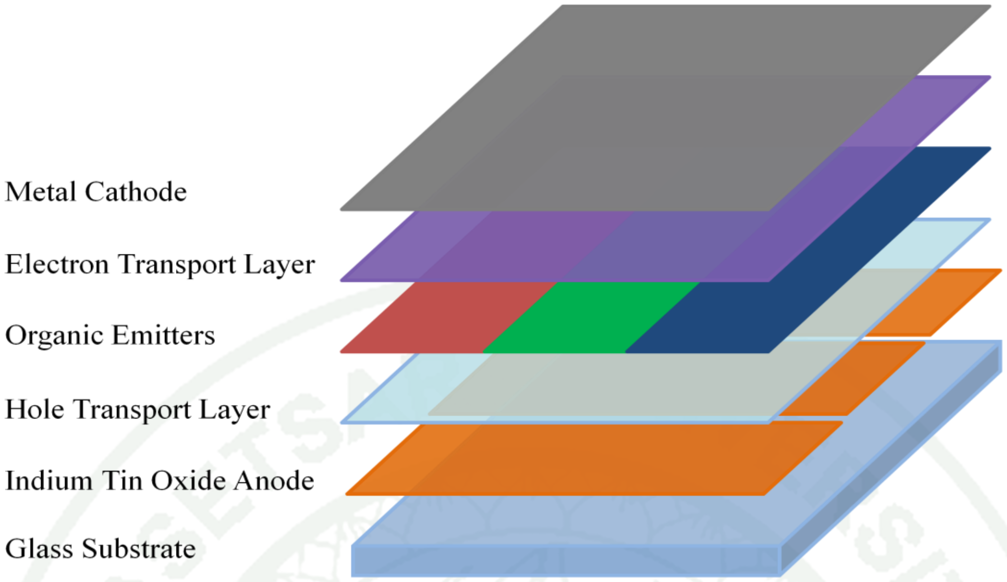

Figure 1 Organic Light Emitting Diode Diagram.

Organic light-emitting diodes (OLEDs) are fabricated as electroluminescent organic film sandwiched between a high work function anode and a low function cathode. When a voltage is applied between anode and cathode, electrons are injected from the cathode into the π*-band (lowest unoccupied molecular orbital, LUMO) of the organic materials, and holes are injected from the anode into the π-band (highest occupied molecular orbital, HOMO). The injected electrons and holes interact within the organic materials film and radiatively decay to produce electroluminescence, which causes electroluminescent light (Figure 2). The emissive organic materials, supplied with an electrical current, can produce full-color display and panel light sources (Sheats *et al*., 1999). For full-color application, it is necessary to have red (620-700 nm), green (500-550 nm) and blue (430-500 nm) emitters with sufficiently high light-emitting efficiencies, low operating voltages and high external quantum efficiency. These three colors of light depend on the type of emissive organic material. The emissive organic materials have π-conjugated system in the structures and they have smaller hole injection barrier than electron injection barrier. Furthermore, the conjugated organic materials or conjugated polymer with low HOMO-LUMO energy level, by increasing the electron affinity, have been used as materials for OLED device.

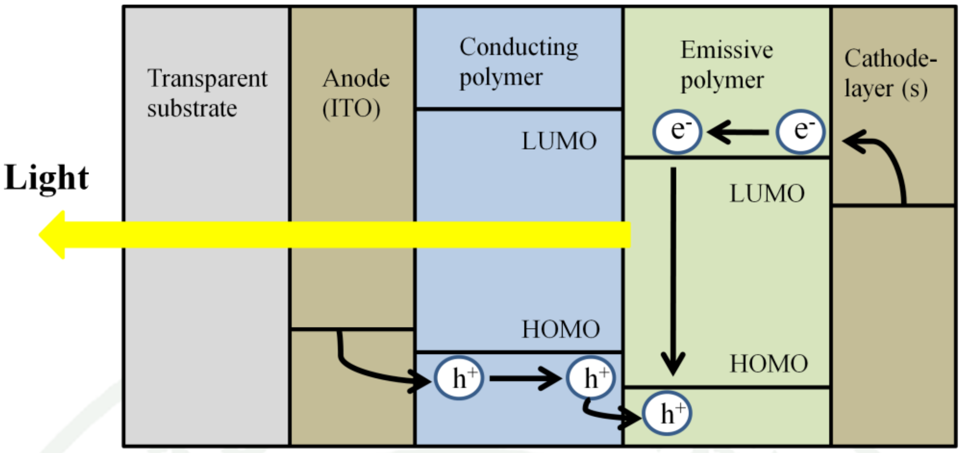

Figure 2 Process of organic light-emitting diodes (OLED).

Much effort has been undertaken recently to develop flexible and tunable light-emitting diodes (LEDS) from conjugated polymers. Many conjugated polymers have been designed and synthesized to develop blue-, green-, and red-light-emitting materials (Belletete *et al.*, 2004). They have some very interesting electronic and optical properties and have been investigated as advanced molecular electronic materials. The properties of the resulting conjugated polymers are a function of the monomeric components of the polymerized moiety, the organic solvent and supporting electrolyte, and the material of the anode.

3,6-Substituted carbazoles have been proved to be effective charge transporting, electroluminescent and host materials with improved thermal and morphological stabilities. Structurally well-defined carbazole derivatives and their chemistry have been studied at length due to their biological activity (Yamashita *et al.*, 1992; Chakraborty *et al.*, 1997). However, in the last decade the amorphous and film-forming compounds have attracted much attention in terms of molecular electronic materials (Strohriegl *et al.*, 2003). The carbazole-based compounds demonstrate high thermal, morphological, chemical and environmental stability. Two basic properties of the fully aromatic carbazolyl group are the easy oxidizability of nitrogen atom and its ability to transport positive charge centers via the radical cation species. Such derivatives are finding various applications in photoconductors (Law, 1993; Yang *et al.*, 2000; Lamansky *et al.*, 2001), field effect transistors

(Dimitrakopoulos *et al.*, 2004; Katz, 2004) and in particular as organic photorefractive materials (Ostroverkhova *et al.*, 2004) and components of electroluminescent devices (Shirota, 2000; Mitshke *et al.*, 2000).

The synthetic efforts have been made toward small bandgap conjugated polymers by adding electron donor or electron acceptor groups the energy gaps (E_g) of conjugated polymers can be reduced to below 1 eV while sustaining good stability. Theoretical calculations have also proved to be of importance for these studies because of the various limitations of experiments. Due to the high level of disorder associated with most of these materials, structural information could not be obtained easily by experimentally. Therefore, theoretical studies are used to investigate energy gap control. Theoretical investigations have been proven to be an important tool for studying the relationships between electronic structures and optical properties of the π-conjugated materials. This helps in understand a fundamental of the conformational analysis, electronic and optical characteristics of known materials and in guiding the experimental efforts toward novel compound with enhanced characteristics. The theoretical quantity of energy gap for direct comparison with the experimental energy gap (E_g) should be the transition (or excitation) energy from the ground state to the first dipole-allowed excited state (Zhu *et al.*, 2004). The energy gap (E_g) in an extended system is defined as the difference between the highest occupied molecular orbital (HOMO) and the lowest unoccupied molecular orbital (LUMO). Theoretical approaches are available to calculate the extrapolation energy gap for increasing longer oligomers, and extrapolation to infinite chain length is followed. A distinct advantage of this approach is that it can provide the convergence behavior of the structural and electronic properties of oligomers. In practice both the oligomers extrapolation and the polymer approaches are generally considered to be complementary to each other in our understanding of the properties of polymers.

For the quantum chemical calculation on both the ground states and excited states, theoretical methods have been applied to different conjugated polymer systems (Huang *et al.*, 2001; Corral *et al.*, 2000; Poolmee *et al.*, 2005; Meeto *et al.*, 2008). In particular, the density function theory (DFT) method is able to describe the geometry molecules, as well as their energetic, in a satisfactory manner (Grozema *et al*., 2005). Hybrid exchange correlation functionals are widely used in the DFT formalism, to get a better fit with experiments. Popular forms of hybrid DFT methods, including Becke's three parameter hybrid functional (Becke., 1993) using the Lee Yang Parr (LYP) (Lee *et al*., 1988) correlation functional (B3LYP). There are many applications of hybrid DFT in conjugated polymers, which gives acceptable results for the geometry and HOMO-LUMO gaps of oligomers for some hetero-type conjugated polymers (Hutchison *et al*., 2002). Many researchers focus on TDDFT method in order to investigate the electronic properties with geometry relaxation effects in excited states (Jacquemin and Perpète, 2006). In 2006, Saha and coworker pointed out that conventional TDDFT with the B3LYP functional should be used carefully, because it can provide inaccurate estimates of the chain length dependence of π-π* excitation energies for these molecules with long π-conjugated chains. Nowadays, TDDFT still has some limitations, even though it can be helpful in understanding fundamentals of the electronic and optical characteristics of conjugated polymers and guiding the experimental efforts toward compounds with enhanced characteristics.

Thus, the main objectives of this work are to synthesize and characterize the 9-octyl-3,6-di(thiophen-2-yl)-carbazole and derivatives. The effect of substituents on structures and electronic properties with electron donating and withdrawing groups are investigated. In addition, quantum chemical calculations are study on the structural, electronic and optical properties of the 9-octyl-3,6-di(thiophen-2-yl)-carbazole and derivatives by density functional theory method to compare between the experimental and theoretical results.

OBJECTIVES

1. To synthesize and characterize the 9-octyl-3,6-di(thiophen-2-yl)-carbazole derivatives.

2. To investigate the 9-octyl-3,6-di(thiophen-2-yl)-carbazole derivatives by quantum chemical calculations.

3. To compare the absorption and emission properties between the quantum chemical calculations molecules and experimental results of the 9-octyl-3,6-di(thiophen-2-yl)-carbazole derivatives.

LITERATURE REVIEW

The molecular origin of the electrical and optical properties presented by polythiophene, polyfluorene and other polyconjugated materials requires the intramolecular delocalization of the π-electrons along the conjugated chain. The degree of planarity has a direct influence on the effective conjugation length as well as the width of the π-bands including the optical band gap. Thus the knowledge of the backbone conformation of the polymers is very important. For example, it is responsible for the thermochromism that polythiophenes (Cesare *et al*., 1997), poly fluorenes (Blondin *et al*., 2000) and other polymers (Leclerc *et al.*, 2001) exhibit in solution and in the solid state and can also be used to control both electrical and optical properties of these materials. Therefore conformational analysis studies on dimeric species which serve as a model for polymeric systems are of fundamental importance once it can provide useful information that can enable us to understand the behavior of the real polymer (Belletete *et al.*, 2004).

In synthetic chemistry, carbazole has been extensively exploited as a convenient building block for the development of biologically active compounds (Link *et al*., 1996), photorefractive materials (Zhang *et al*., 1998) and more recently, liquid crystals (Darbaro *et al*., 1997). The carbazole molecular moiety has been exploited in organic photorefractive materials in both polymeric and low-molecular weight systems (Zhang *et al.*, 1997). Introduction of substituents on the 3- and 6-positions of carbazole represents a possible approach for designing carbazole-based photorefractive materials. Additionally, by extending the central aromatic core and introducing flexible alkyl chains into the periphery of the molecular architecture as required for liquid crystals design it should be possible to obtain a structure that is both photorefractive and liquid crystalline and, therefore, superior for photorefractive applications (Belloni *et al.*, 2005). A synthetic route to the synthesis of 3,6-bis (thiophen-2-yl)-9-(2-ethyl-hexyl)carbazole by Suzuki cross-coupling (Promarak *et al*., 2007). Alkyl carbazole was used and synthesized. The alkyl substituents would provide good solubility to the desired products in common organic solvents.

Carbazole is a prototypical organic molecule that has shown potential for technological applications (Romero *et al.,* 1996). The synthesis and application of carbazole derivatives has been of great interest for chemists and materials scientists due to their intrinsic photophysical properties, high thermal stabilities, photochemical stabilities (Shi *et al*., 2010; Morin *et al*., 2002) and redox properties i.e., they exhibit relatively intense luminescence and undergo reversible oxidation processes making them suitable as hole transporting mobility. Two basic properties of the fully aromatic carbazolyl group are the easy oxidizability of nitrogen atom and its ability to transport positive charge centers via the radical cation species (Grigalevicius *et al.,* 2006). Such derivatives are finding various applications in photoconductors (Law *et al*., 1993) field effect transistors (Dimitrakopoulos *et al.,* 2002) and in particular as organic photorefractive materials and components of electroluminescent devices (Shirota *et al.,* 2000). Carbazole derivatives are also widely used as building blocks for potential organic semiconductors, especially for organic light-emitting diodes (Feng *et al.,* 2006). Its ring can be easily functionalized by covalently linked to other molecules (Shi *et al.,* 2010).

The ground and excited states of covalently linked 2-carbazole-based dimer were investigated by theoretical methods and by UV-vis and fluorescence spectroscopy. Geometry optimizations of the ground state of *N*,*N*'-diethyl-2,2'-bicarbazole (CC), 2-(*N*-ethylcarbazol-2-yl)-thiophene (CT), and 2-(*N*-ethylcarbazol-2-yl)-9,9-diethylfluorene (CFl) were carried out at the restricted Hartree-Fock level (RHF/6-31G(d)). The derivative is non-planar in their ground electronic states (Belletete *et al*., 2004). The ground state optimized structures and energies are obtained using the molecular orbital theory and the density functional theory (DFT). The potential energy curves of the dimers are also obtained. All molecules are non-planar in their electronic ground states (Gong *et al.,* 2008). The $S_2 \leftarrow S_0$ electronic transition possesses much larger oscillator strength and is polarized along the x-axis. Electronic transition energies from the relaxed excited states have been obtained from ZINDO/S calculations performed on the optimized geometries of S_1 and S_2. It is found that the electronic transition energies from the first relaxed excited state are close to those determined experimentally from the fluorescence spectra recorded in *n*-

hexane. CT possesses a shorter conjugation length (10.6 Å) than CC (14.8 Å). Thus, this behavior shows that a thiophene ring possesses better electron donor properties than a carbazole unit (Belletete *et al*., 2004).

Promarak *et al* (2007) studied the synthesis of novel N-carbazole end-capped π-conjugated bisthiophenyl derivatives by Suzuki cross-coupling and Ullmann reactions. They investigated the optical, thermal and electrochemical properties. The results were shown that UV–vis absorption spectra displayed bathochromic shift with respect to their conjugated backbones and photoluminescence spectra showed emission maxima in the blue region. Thermal analysis revealed that they are thermally stable semi-crystalline and amorphous materials and all molecules exhibited good electrochemical stability.

The preparation of a carbazole copolymer alternating 3,6-linked-9-alkyl-9H-carbazole units and 2,7-linked-3,6-dimethyl 9alkyl-9H-carbazole units has been achieved using Suzuki cross-coupling method. The characteristic polymer was stable up to 420 °C and has a band gap of 3.2 eV. Fluorescence studies indicated that the polymer has a particularly narrow emission band around 400 nm (Pickup *et al.*, 2009). The solution spectra are blue shifted in comparison with those from poly(9-alkyl-9H-carbazole-3,6-diyl)s (≈425 nm) (Iraqi and wataru., 2004) and are similar to those of poly(3,6-dimethyl-9-alkyl-9H-carbazole-2,7-diyl)s (≈397 nm) (Iraqi *et al.*, 2006).

In 2006, Doskocz and coworker investigated on the ground-state geometries of the studied monomers and short oligomers were optimized by applying the density functional theory (DFT) using the B3LYP/6-311G(d,p). The calculations were performed for a selected group of compounds based on carbazole and fluorene substituted symmetrically by thiophene, ethylenodioxythiophene, furane, and pyrrole. Studies of the variation in the properties are a function of the chemical composition of the central fragment and the external rings. They were found that the substitution in positions 2,7 of the central fragment leads to a smaller energy gap compared to its analogue with the substitution in the 3,6 positions. The smallest HOMO-LUMO gap is found in derivatives of ethylenedioxythiophene.

In 2007, Suramitr and coworker investigated on conformation and vertical excitation energies of carbazole-based molecules were carried out by B3LYP calculations with 6-31G, 6-31G(d) and 6-311G(d,p) basis set. Carbazole-based molecules combined with five-membered (Cz-co-Thiophene $(\text{Cz-co-Th})_N$ and Cz-co-Furan $(\text{Cz-co-F})_N$) and six-membered (Cz-co-Fluorene $(\text{Cz-co-Fl})_N$ and Cz-co-Phenyl $(\text{Cz-co-P})_N$) aromatic rings. The analyses of potential energy surfaces and torsional angles for carbazole-based oligomers give that these copolymerized with five-membered aromatic rings are more planar than those copolymerized with six-membered ring. The excitation energies calculated by TD-B3LYP are comparing with those of TD-PBE1PBE and agree with experimental data. For carbazole-based oligomers were found that the vertical excitation with the S_1 state plays a major role. The behavior of these molecules depends on the number of chain length and this can be explained by the HOMO-LUMO orbital.

MATERIALS AND METHODS

Synthesis and Characterization

1. Materials

- 5-Acetyl-2-thiopheneboronic acid ($C_6H_7BO_3S$)
- 1-Bromooctane ($CH_3(CH_2)_7Br$)
- 1-Bromo-2,5-pyrrolidinedione (NBS, $C_4H_4BrNO_2$)
- 9H-carbazole ($C_{12}H_9N$)
- Dimethyl sulfoxide (DMSO, C_2H_6OS)
- Disodium carbonate (Na_2CO_3)
- *N*,*N*-dimethylmethannamide (DMF, C_3H_7NO)
- Ethanol (C_2H_5OH)
- Ether
- 5-Formyl-2-thiopheneboronic acid ($C_5H_5BO_3S$)
- Hexane (C_6H_{14})
- Magnesium sulfate ($MgSO_4$)
- 5-Methyl-2-thiopheneboronic acid ($C_5H_5BO_3S$)
- Sodium hydroxide (NaOH)
- Tetrahydrofuran (THF, C_4H_8O)
- Tetrakis(triphenylphosphine)palladium ($Pd(PPh_3)_4$)
- 2-Thienylboronic acid ($C_4H_5BO_2S$)

2. Instruments

^1H- NMR analyses was carried out using a VARIAN ^{UNITY} INOVA spectrometer which operated at 400.00 MHz for ^1H in deuterated chloroform ($CDCl_3$) with tetramethysilane (TMS) as an internal reference. UV analysis was done with Perkin Elmer Lambda 35 UV-Vis spectrophotometer, using a quartz cell with 1 cm path length. Fluorescence analysis was obtained using Perkin Elmer Instruments LS55 fluorescence spectrophotometer. Thermogravimetric analysis (TGA) was performed under nitrogen atmosphere at heating rate of 10 °C/min on a Perkin Elmer TGA-7 thermal analyzer.

3. Synthesis

The solid state structure of 9-octyl-3,6-di(thiophen-2-yl)-carbazole derivatives have been investigated (Figure 3).

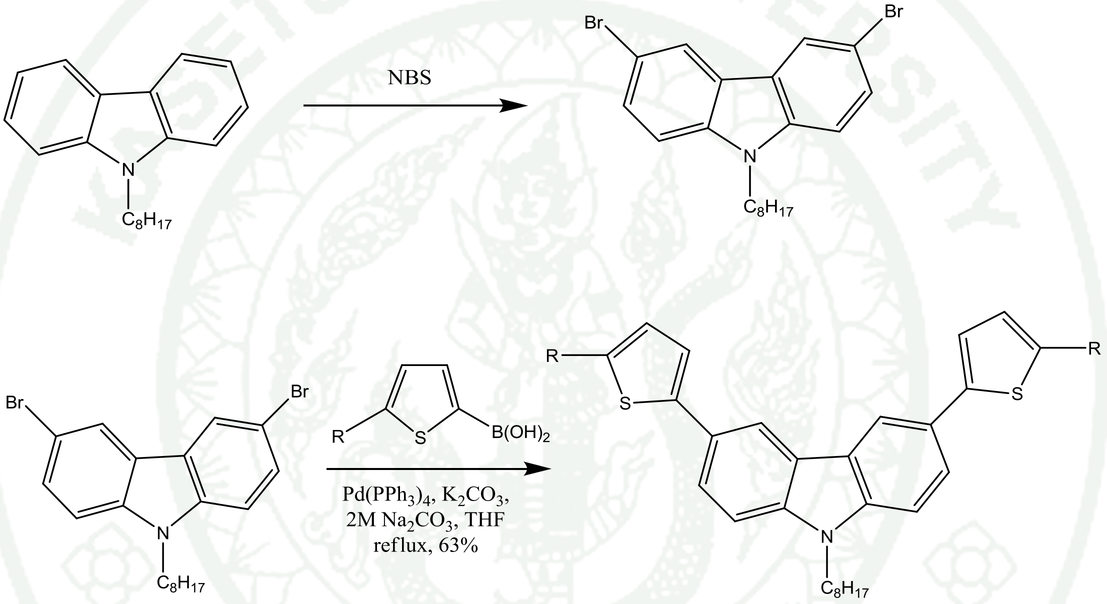

Figure 3 Synthesis of 9-octyl-3,6-di(thiophen-2-yl)-carbazole derivatives. (R = -CH_3, -$COCH_3$ and -CHO)

3.1 Synthesis of 3,6-dibromo-9H-carbazole (A2)

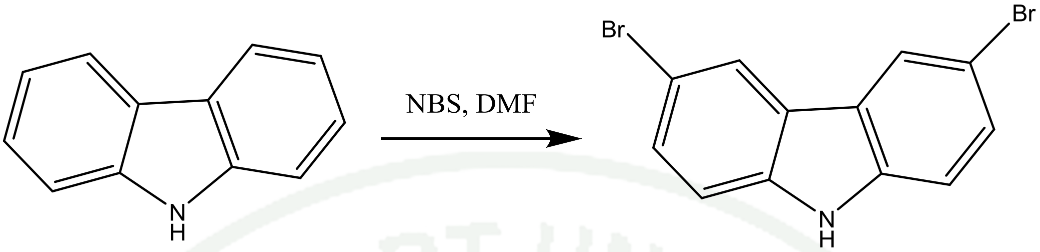

(A1) (A2)

Carbazole (A1) (35.65 g, 0.213 mol) was dissolved in dimethylformamide (DMF) (400 ml) in a 1000 ml three-necked flask. After the solution was cooled to 0 °C, *N*-bromosuccinimide (NBS) (75.89 g, 0.426 mol) in DMF was added dropwise through a dropping funnel. The mixture was allowed to warm to room temperature and stirred for an additional 2 h. The mixture was then poured into water (2000 ml). The white precipitates collected by filtration were recrystallized from ethanol to give colorless crystals.

^{1}H-NMR (DMSO, δ *ppm*): 7.45 (2H, dd, -Ar-H), 7.52 (2H, dd, -Ar-H), 8.41 (2H, dd, -Ar-H), 11.57 (1H, s, -NH)

3.2 Synthesis of 3,6-Dibromo-9-octyl-carbazole (A3)

To a 250-mL threenecked flask containing 3,6-dibromo-9H-carbazole (A2) (16.25 g, 50 mmol) in DMSO (100 ml) were added 1-bromooctane (14.48 g, 75 mmol) and 50% NaOH solution (50 ml). The mixture was stirred at room temperature for 4 h, after which ether (100 ml) and deionized water (100 ml) were added. The organic layer was washed with brine and water and dried over $MgSO_4$. After filtration and evaporation of the solvent, the resulting solid was dissolved in hexane and purified by passing through a silica gel column. Recrystallization from heptanes produced white crystals.

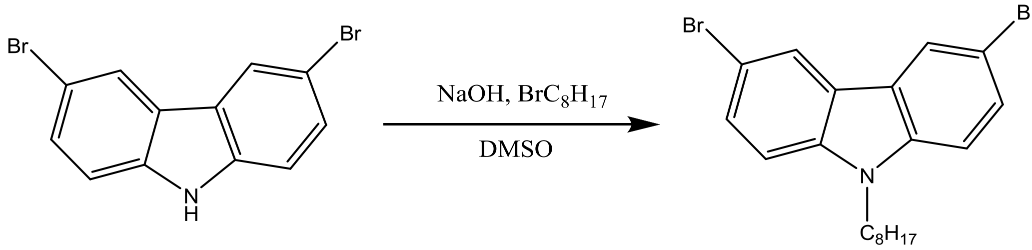

(A2) (A3)

^1H-NMR ($CDCl_3$, δ *ppm*): 0.77-0.80 (3H, t, $-CH_3$), 1.16–1.23 (12H, m, $-CH_2$), 4.15 (2H, t, $-CH_2$), 7.14 (2H, s, -Ar-H), 7.49 (2H, d, -Ar-H), 8.07 (2H, s, -Ar-H)

3.3 Synthesis of 9-octyl-3,6-di(thiophen-2-yl)-carbazole (Th-3,6Cz-Th-H)

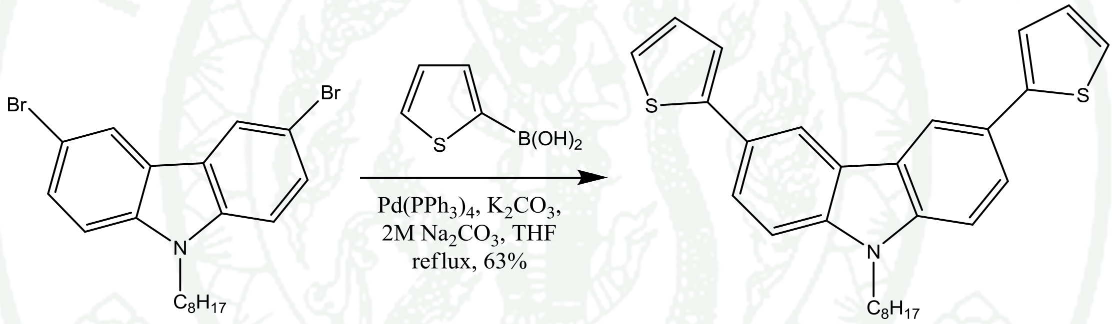

(A3) (Th-3,6Cz-Th-H)

A mixture of 3,6-Dibromo-9-octyl-9H-carbazole (A3) (0.23 g, 0.7 mmol), 2-thiopheneboronic acid (0.2 g, 1.56 mmol), $Pd(PPh_3)_4$ (0.0116 g, 0.01 mmol) and 2 M Na_2CO_3 aqueous solution (15 ml, 30 mmol) in THF (20 ml) was stirred at reflux under N_2 atmosphere for 24 h. Water (150 ml) and CH_2Cl_2 (150 ml) were added. The organic phase was separated, washed with water (150 ml), brine solution (100 ml), dried over anhydrous Na_2SO_4, filtered, and the solvents removed to dryness. Purification by column chromatography using silica gel eluting with hexane gave light green solids.

^1H-NMR ($CDCl_3$, δ *ppm*): 0.88–0.98 (6H, m, $-CH_3$), 1.27–1.47 (8H, m, $-CH_2$), 2.07–2.11 (1H, m, -CH), 4.16 (2H, dd, J=7.8 Hz, J=1.8 Hz, $-CH_2$-N), 7.14 (2H, dd, J=5.1

Hz, J=3.6 Hz, -CH), 7.29 (2H, dd, J=5.1 Hz, J=1.2 Hz, -CH), 7.38–7.40 (4H, m), 7.75 (2H, dd, J=8.4 Hz, J=1.8 Hz, -Ar-H), 8.36 (2H, d, J=1.8 Hz, -Ar-H)

3.4 Synthesis of 3,6-bis(5-methylthiophen-2-yl)-9-octyl-9H-carbazole (Th-3,6Cz-Th-CH_3)

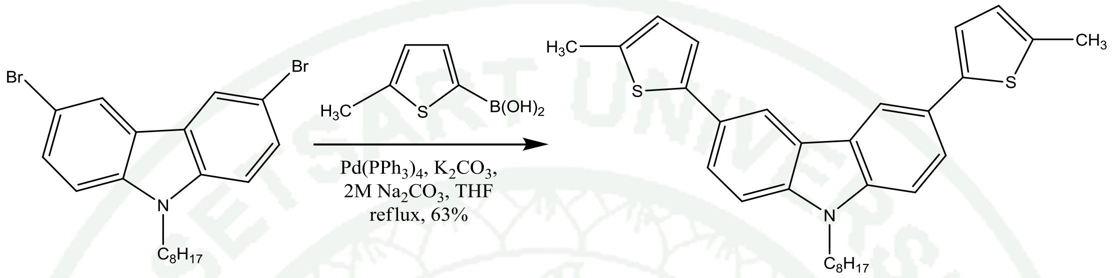

(A3) (Th-3,6Cz-Th-CH_3)

A mixture of 3,6-Dibromo-9-octyl-9H-carbazole (A3) (0.23 g, 0.7 mmol), 5-Methyl-2-thienylboronic acid (0.2215 g, 1.56 mmol), $Pd(PPh_3)_4$ (0.0116 g, 0.01 mmol) and 2 M Na_2CO_3 aqueous solution (15 ml, 30 mmol) in THF (20 ml) was stirred at reflux under N_2 atmosphere for 24 h. Water (150 ml) and CH_2Cl_2 (150 ml) were added. The organic phase was separated, washed with water (150 ml), brine solution (100 ml), dried over anhydrous Na_2SO_4, filtered, and the solvents removed to dryness. Purification by column chromatography using silica gel eluting with hexane.

^{1}*H*-NMR ($CDCl_3$, δ *ppm*): 0.88 (3H, m, -CH_3), 1.25–1.73 (12H, m, -CH_2), 2.61 (6H, s, -CH_3), 6.60 (2H, d, -CH), 6.70 (2H, d, -CH), 7.34 (4H, m, -Ar-H), 7.58 (2H, s, -Ar-H)

3.5 Synthesis of 5,5’-(9-octyl-carbazole-3,6-diyl)-dithiophene-2-carbalde- hyde (Th-3,6Cz-Th-CHO)

A mixture of 3,6-Dibromo-9-octyl-9H-carbazole (A3) (0.23 g, 0.7 mmol), 5-Formyl-2-thiopheneboronic acid (0.243 g, 1.56 mmol), $Pd(PPh_3)_4$ (0.0116 g, 0.01 mmol) and 2M Na_2CO_3 aqueous solution (15 ml, 30 mmol) in THF (20 ml) was stirred at reflux under N_2 atmosphere for 24 h. Water (150 ml) and CH_2Cl_2 (150 ml) were added. The organic phase was separated, washed with water (150 ml), brine solution (100 ml), dried over anhydrous Na_2SO_4, filtered, and the solvents removed to dryness. Purification by column chromatography using silica gel eluting with hexane.

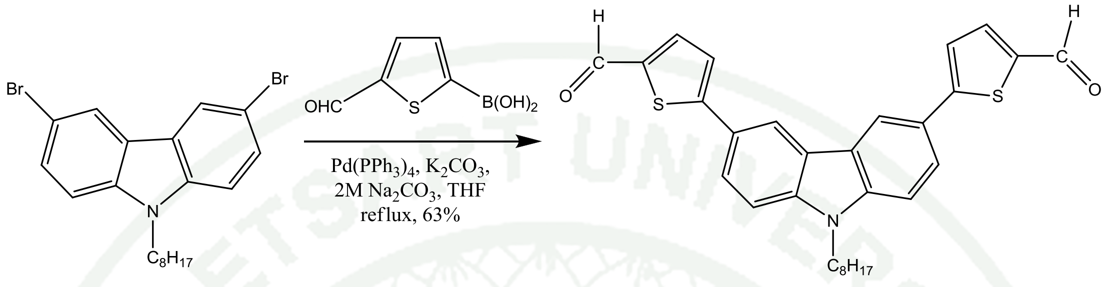

(A3) (Th-3,6Cz-Th-CHO)

^1H-NMR ($CDCl_3$, δ *ppm*): 0.79 (3H, m, $-CH_3$), 1.29 (8H, m, CH_2), 1.31 (2H, m, $-CH_2-CH_3$), 4.16 (2H, t, $-CH_2-N$), 7.58 (2H, d, -CH), 7.88 (2H, dd, -CH), 7.91 (1H, d, -CH), 7.99-8.00 (4H, d, -CH), 9.84 (2H, s, H-C=O)

3.6 Synthesis of 1,1’-(5,5’-(9-octyl-carbazole-3,6-diyl)-bis-(thiophene-5,2-diyl))-diethanone (Th-3,6Cz-Th-$COCH_3$)

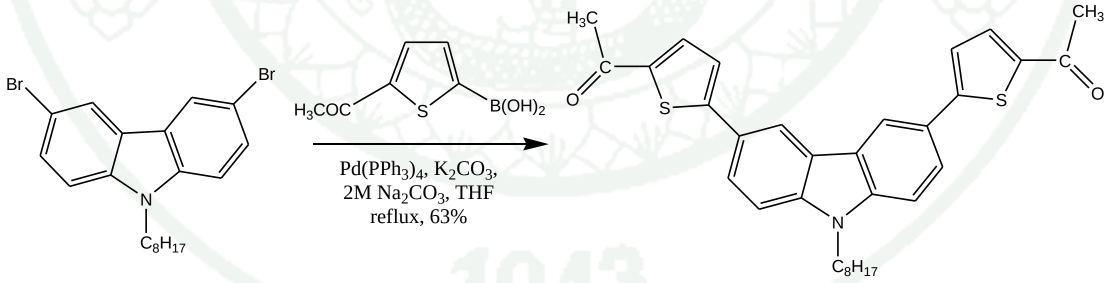

(A3) (Th-3,6Cz-Th-$COCH_3$)

A mixture of 3,6-Dibromo-9-octyl-9H-carbazole (A3) (0.23 g, 0.7 mmol), 5-Acetyl-2-thienylboronic acid (0.265 g, 1.56 mmol), $Pd(PPh_3)_4$ (0.0116 g, 0.01 mmol) and 2 M Na_2CO_3 aqueous solution (15 ml, 30 mmol) in THF (20 ml) was stirred at reflux under N_2 atmosphere for 24 h. Water (150 ml) and CH_2Cl_2 (150 ml) were added. The organic phase was separated, washed with water (150 ml), brine solution (100 ml), dried over anhydrous Na_2SO_4, filtered, and the solvents removed to dryness.

Products were purified by column chromatography using silica gel eluting with hexane.

^{1}H-NMR ($CDCl_3$, δ *ppm*): 0.79 (3H, m, $-CH_3$), 1.17 (8H, m, $-CH_2$), 1.33 (2H, m, $-CH_2-CH_3$), 1.73 (2H, m, $-CH_2$), 2.49 (6H, s, $-CH_3$), 4.24 (2H, t, $-CH_2-N$), 7.00 (2H, d, -CH), 7.34 (4H, m, -Ar-H), 7.50 (2H, d, -CH), 7.58 (2H, d, -Ar-H)

METHODS OF CALCULATIONS

Quantum Chemical Calculations

Quantum chemical calculation is the application of chemical, mathematical and computational skills to the approximations of chemistry problems. It uses computers to generate information such as properties of structure and dynamic molecular system. It also helps predict before running the actual experiments so that they can be better prepared for making observations. Theoretical studies are an important to approximate the electronic structure determinations, geometry optimizations, frequency calculations, transition structures, protein calculations, electron and charge distributions, potential energy surfaces (PES), rate constants for chemical reactions (kinetics), thermodynamic calculations heat of reactions and energy of activation of molecular system with common computer software. In addition, the experimental cannot be explained with the electron term. Computational quantum chemistry is one of the challenging tasks in calculating the electronic structure and predicting properties of variety of molecules. This approach can be provided molecular models and guide the design of novel molecules.

1. Model of calculation

Starting geometries of 9-octyl-3,6-di(thiophen-2-yl)-carbazole derivatives, 9-octyl-3,6-di(thiophen-2-yl)-carbazole (Th-3,6Cz-Th-H), 1,1’-(5,5’-(9-octyl-carbazol -3,6-diyl)-bis-(thiophene-5,2-diyl))-diethanone) (Th-3,6Cz-Th-$COCH_3$), 3,6-bis(5me-thylthiophen-2-yl)-9-octyl-carbazole (Th-3,6Cz-Th-CH_3), and 5,5’-(9-octyl-carbazole -3,6-diyl)-dithiophene-2-carbaldehyde (Th-3,6Cz-Th-CHO) were constructed by molecular modeling. The molecular structure of Th-3,6Cz-Th-H composed of the two thiophene rings. Th-3,6Cz-Th-CH_3, Th-3,6Cz-Th-$COCH_3$, Th-3,6Cz-Th-CHO are similar structure to that of Th-3,6Cz-Th-H but they are replaced by methyl, acetyl and formyl group on hydrogen atom on the thiophene group. The structures of all molecule as shown in Figure 4 and 5. Then the ground state geometry of their molecules was determined by a full optimization using the density functional theory

(DFT) level. The basis set 6-31G(d) has been used for the geometries optimization. All calculations were performed using the Gaussian 09 program package.

2. Conformation Analysis

In this study, the Th-3,6Cz-Th-H conformation was investigated. The bond length, bond angle and torsion angle were calculated using PBE0 method with 6-31G(d) basis set. The main chain structure (C1-C14 atoms) was considered for conformational analysis of the bond length parameter. The units (∠C3-C4-C5-C6 and ∠C9-C10-C11-C12) were studies with the bond angle and torsion angle which is directly connected to backbone for Th-3,6Cz-Th-H structure. Moreover, the alkyl substituents at N atom play an important role in the solubility and do not affect the electronic structure and optical properties. Therefore, we might neglect the appearance of alkyl group at that position here. Consequently, the models and also the atom number used in this study are shown in Figure 4(a).

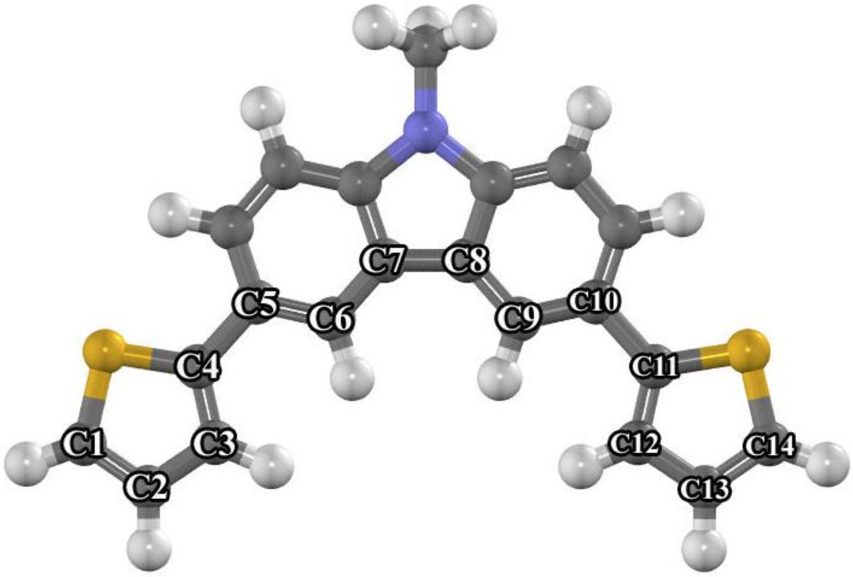

(a)

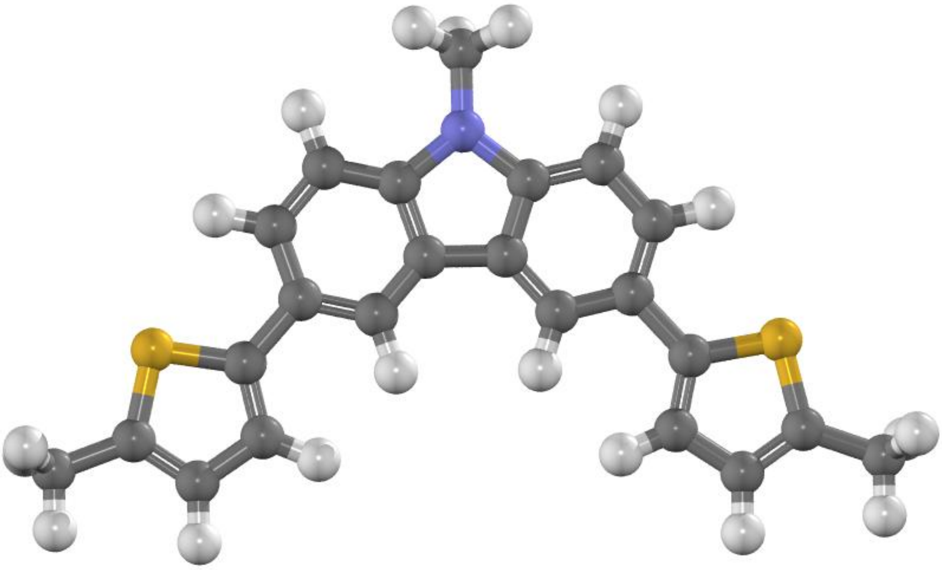

(b)

Figure 4 Schematic diagram of Th-3,6Cz-Th-H (a) and Th-3,6Cz-Th-CH_3 (b) structures.

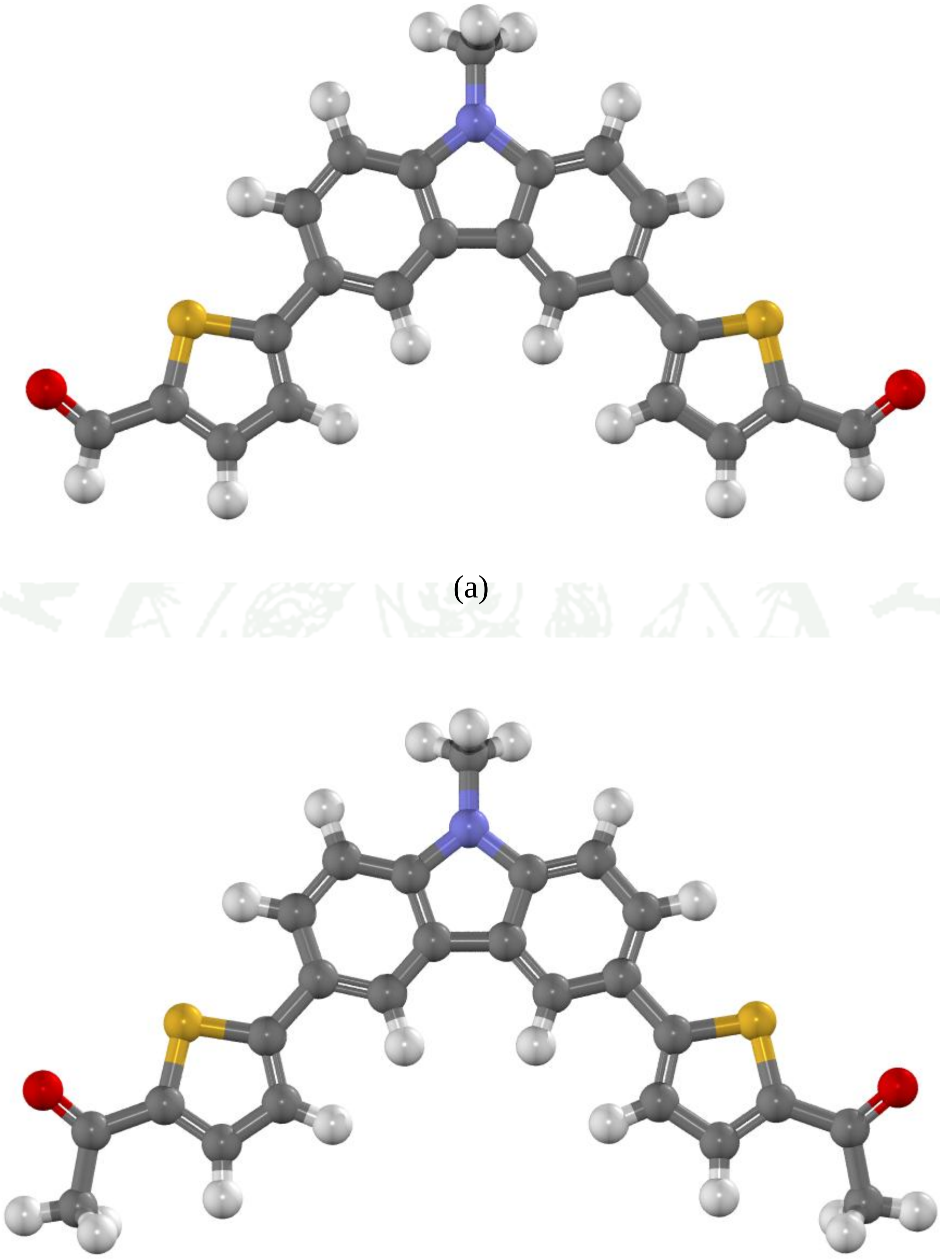

(a)

(b)

Figure 5 Schematic diagram of Th-3,6Cz-Th-CHO (a) and Th-3,6Cz-Th-$COCH_3$ (b) structures.

3. Electronic Properties

3.1 Absorption and Emission properties

The electronic transitions were calculated by time-dependent density function theory (TDDFT) method employing the basis set 6-311G(d,p) based on the PBE0/6-31G(d) optimized geometries in the Gaussian 09 program packages. The excitation energies and emission transition energies calculations of all molecules have been carried out at TD-PBE0/6-311G(d,p) level by using Gaussian 09 program packages.

3.2 Fluorescence Energy and Radiative lifetime

The fluorescence energy as the emission transition energies was obtained from the vertical de-excitation at the optimized first singlet excite state using TD-PBE0/6-311G(d,p) method. Radiative lifetime can be calculated on the fluorescence energy and oscillator strengths according to the following formula (Bransden and Joachain, 1983).

$$\tau = \frac{c^3}{2(E_{flu})^2 f}$$

Where c is the velocity of light, E_{flu} is the fluorescence transition energy and f is oscillator strength. Fluorescence or radiative lifetime provides information useful in discrimination of particles which the long conjugated system leads to a decrease of lifetime.

RESULTS AND DISCUSSION

Synthesis and Characterization

1. Synthesis

1.1 Synthesis of 9-octyl-3,6-di(thiophen-2-yl)-carbazole (Th-3,6Cz-Th-H)

The syntheses of 9-octyl-3,6-di(thiophen-2-yl)-carbazole (Th-3,6Cz-Th-H) was started by treat carbazole with N-bromosuccinimide (NBS) as a brominating reagents to give the corresponding dibromo compound. 3,6-dibromo-9H-carbazole (A2) can be easily obtained using dimethylformamide (DMF) at 0 °C. The compound 3 (A3) was substituted with the alkyl group with bromooctane (BrC_8H_{17}) in dimethyl sulfoxide (DMSO). The Th-3,6Cz-Th-H was obtained by coupling of the resultant dibromo compound with 2-thiopheneboronic acid under Suzuki reaction to afford the product in 29.78% yield. This synthesis method of Th-3,6Cz-Th-H was prepared consisting of a central carbazole core disubstituted with two thiophene rings.

The spectrum of ^1H-NMR measurement was shown in Appendix A. The ^1H-NMR spectrum of Th-3,6Cz-Th-H was easily obtained because it can be dissolved in *d*-chloroform ($CDCl_3$) at room temperature. The ^1H-NMR spectrum exhibits the chemical shift of alkyl side chain in the region of 0.88-4.16 *ppm*. The aromatic group (carbazole ring) signal appears at 7.40-8.36 *ppm*. The thiophene-H shows douplet of douplet (dd) at 7.29 *ppm* with a coupling constant of 5.1 amd 1.2 Hz. The thiophene protons signals are attributed to thienyl proton adjacent sulfur atom on thiophene ring.

1.2 Synthesis of 3,6-bis(5-methylthiophen-2-yl)-9-octyl-9H-carbazole (Th-3,6 Cz-Th-CH_3)

The syntheses of 3,6-bis(5-methylthiophen-2-yl)-9-octyl-9H-carbazole (Th-3,6Cz-Th-CH_3) was started by treat carbazole with N-bromosuccinimide (NBS) as a brominating reagents to give the corresponding dibromo compound. 3,6-dibromo-

9H-carbazole (A2) can be easily obtained using dimethylformamide (DMF) at 0 °C. The compound 3 (A3) was substituted with the alkyl group with bromooctane (BrC_8H_{17}) in dimethyl sulfoxide (DMSO). The Th-3,6Cz-Th-CH_3 was obtained by coupling of the resultant dibromo compound with 5-Methyl-2-thienylboronic acid under Suzuki reaction to afford the product as solid in 22.07% yield. This synthesis method of Th-3,6Cz-Th-CH_3 was prepared consisting of a central carbazole core disubstituted with two thiophene rings that substituent at 5-position of thiophene rings with methyl group.

The spectrum of ^1H-NMR measurement was shown in Appendix A. The ^1H-NMR spectrum of Th-3,6Cz-Th-CH_3 was easily obtained because it can be dissolved in *d*-chloroform ($CDCl_3$) at room temperature. The ^1H-NMR spectrum exhibits the chemical shift of alkyl side chain in the region of 0.88-1.73 *ppm*. The aromatic group (carbazole ring) signal appears at 7.34-7.58 *ppm*. The thiophene-H shows douplet (d) at 6.70 *ppm*. The methyl group (-CH_3) signal appears at 2.61 *ppm*. The thiophene protons signals are attributed to thienyl proton adjacent sulfur atom on thiophene ring.

1.3 Synthesis of 5,5’-(9-octyl-carbazole-3,6-diyl)-dithiophene-2-carbaldehyde (Th-3,6Cz-Th-CHO)

The syntheses of 5,5’-(9-octyl-carbazole-3,6-diyl)-dithiophene-2-carbaldehyde was started by treat carbazole with N-bromosuccinimide (NBS) as a brominating reagents to give the corresponding dibromo compound. 3,6-dibromo-9H-carbazole (A2) can be easily obtained using dimethylformamide (DMF) at 0 °C. The compound 3 (A3) was substituted with the alkyl group with bromooctane (BrC_8H_{17}) in dimethyl sulfoxide (DMSO). The Th-3,6Cz-Th-CHO was obtained by coupling of the resultant dibromo compound with 5-Formyl-2-thiopheneboronic acid under Suzuki reaction to afford the product as solid in 31.41% yield. This synthesis method of Th-3,6Cz-Th-CHO was prepared consisting of a central carbazole core disubstituted with two thiophene rings and substituent at 5-position of thiophene rings with formyl group.

The spectrum of ^1H-NMR measurement was shown in Appendix A. The ^1H-NMR spectrum of Th-3,6Cz-Th-CHO was easily obtained because it can be dissolved in *d*-chloroform ($CDCl_3$) at room temperature. The ^1H-NMR spectrum exhibits the chemical shift of alkyl side chain in the region of 0.79-4.16 *ppm*. The aromatic group (carbazole ring) signal appears at 7.58-7.88 *ppm*. The thiophene-H shows douplet (d) at 7.91 *ppm*. The formyl group (CHO) signal appears at 9.84 *ppm*. The thiophene protons signals are attributed to thienyl proton adjacent sulfur atom on thiophene ring.

1.4 Synthesis of 1,1’-(5,5’-(9-octyl-carbazole-3,6-diyl)-bis-(thiophene-5,2diyl))-diethanone (Th-3,6Cz-Th-$COCH_3$)

The syntheses of 1,1’-(5,5’-(9-octyl-carbazole-3,6-diyl)-bis-(thiophene-5,2-diyl))-diethanone (Th-3,6Cz-Th-$COCH_3$) was started by treat carbazole with N-bromosuccinimide (NBS) as a brominating reagents to give the corresponding dibromo compound. 3,6-dibromo-9H-carbazole (A2) can be easily obtained using dimethylformamide (DMF) at 0 °C. The compound 3 (A3) was substituted with the alkyl group with bromooctane (BrC_8H_{17}) in dimethyl sulfoxide (DMSO). The Th-3,6Cz-Th-$COCH_3$ was obtained by coupling of the resultant dibromo compound with 5-Acetyl-2-thienylboronic acid under Suzuki reaction to afford the product as solid in 56.63% yield. This synthesis method of Th-3,6Cz-Th-$COCH_3$ was prepared consisting of a central carbazole core disubstituted with two thiophene rings that substituent at 5-position of thiophene rings with acetyl group.

The spectrum of ^1H-NMR measurement was shown in Appendix A. The ^1H-NMR spectrum of Th-3,6Cz-Th-$COCH_3$ was easily obtained because it can be dissolved in *d*-chloroform ($CDCl_3$) at room temperature. The ^1H-NMR spectrum exhibits the chemical shift of alkyl side chain in the region of 0.79-1.33 *ppm*. The aromatic group (carbazole ring) signal appears at 7.34 and 7.58 *ppm*. The thiophene-H shows douplet (d) at 7.00 and 7.50 *ppm*. The acetyl group ($COCH_3$) signal appears at 2.55 *ppm*. The thiophene protons signals are attributed to thienyl proton adjacent sulfur atom on thiophene ring.

2. Absorption Properties

The absorption spectra of Th-3,6Cz-Th-H, Th-3,6Cz-Th-CH_3, Th-3,6Cz-Th-CHO and Th-3,6Cz-Th-$COCH_3$ in dichloromethane solution are depicted in Figure 6. The λ_{max} of UV-vis spectra for Th-3,6Cz-Th-H are 252 and 302 nm, the maximum absorption of Th-3,6Cz-Th-CH_3 occur at 298 nm, the maximum absorption of Th-3,6Cz-Th-$COCH_3$ occur at 318, 356 and 365 nm as red shifts with a shoulder, the maximum absorption of Th-3,6Cz-Th-CHO occur at 250 and 393 nm as red shifts with a shoulder. The compound of Th-3,6Cz-Th-$COCH_3$ and Th-3,6Cz-Th-CHO are bathochromic shifts in absorption, as compared to Th-3,6Cz-Th-H, is presumably due to the acetyl group and formyl group which are electron withdrawing groups on the thiophene ring. In addition, there are two main peaks in UV-vis spectra of both compounds. One is due to the π-π* transition of delocalized π electron along the conjugated main chain in long wavelength and another is due to the n-π* electron transition to the side chain in short wavelength.

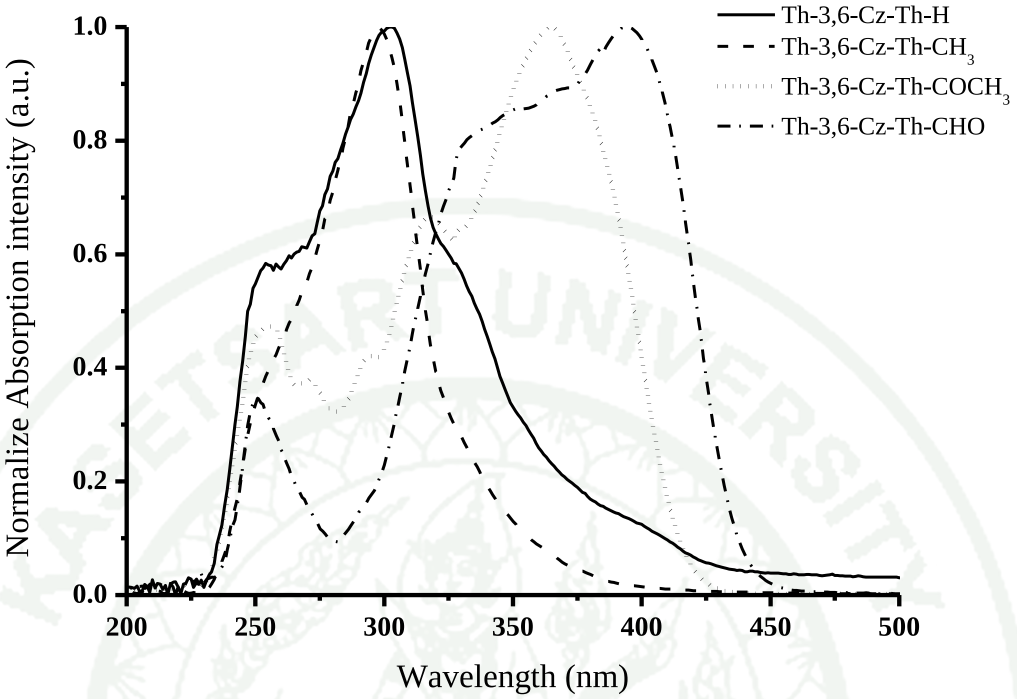

Figure 6 Absorption spectra of Th-3,6Cz-Th-H, Th-3,6Cz-Th-CH_3, Th-3,6Cz-Th-$COCH_3$ and Th-3,6Cz-Th-CHO in CH_2Cl_2 solution.

The low energetic edge of absorption spectrum of Th-3,6Cz-Th-H is 302 nm, which corresponds to a band gap (E_g) of 4.10 eV. While the absorption onset for Th-3,6Cz-Th-CH_3 is 298 nm, corresponding to a band gap (E_g) of 4.16 eV, the absorption onset for Th-3,6Cz-Th-$COCH_3$ is 365 nm, corresponding to a band gap (E_g) of 3.39 eV, the absorption onset for Th-3,6Cz-Th-CHO is 393 nm, corresponding to a band gap (E_g) of 3.16 eV, as summarized in Table 1. Th-3,6Cz-Th-CHO shows lower band gap than Th-3,6Cz-Th-H, Th-3,6Cz-Th-CH_3, Th-3,6Cz-Th-$COCH_3$ as decreasing disorder in the conjugated system due to steric hindrance of the electron-withdrawing formyl group effect. These results could conclude that there is a stronger interchain interaction in Th-3,6Cz-Th-CHO, which leads to more coplanar backbone structure than that Th-3,6Cz-Th-H, Th-3,6Cz-Th-CH_3, Th-3,6Cz-Th-$COCH_3$ structure.

Table 1 Optical data of Th-3,6Cz-Th-H, Th-3,6Cz-Th-CH_3, Th-3,6Cz-Th-$COCH_3$, and Th-3,6Cz-Th-CHO measured in dichloromethane solution

Compound	Absorption		Fluorescence		
	λ_{max} (nm)	E_g (eV)[b]	λ_{max} (nm)	E_g (eV)[b]	Φ_F
Th-3,6Cz-Th-H	302	4.10	405	3.06	0.25
Th-3,6Cz-Th-CH_3	298	4.16	356	3.48	0.20
Th-3,6Cz-Th-$COCH_3$	365	3.39	457	2.71	0.57
Th-3,6Cz-Th-CHO	393	3.16	475	2.61	0.79

[a] Measured in a CH_2Cl_2 solution.

[b] Estimated from the wavelength (E_g=1240/λ_{max})

3. Emission Properties

The emission spectra of Th-3,6Cz-Th-H, Th-3,6Cz-Th-CH_3, Th-3,6Cz-Th-$COCH_3$ and Th-3,6Cz-Th-CHO in dichloromethane at room temperature are shown in Figure 7. The maximum wavelength of emission spectra of Th-3,6Cz-Th-H is 405 nm. Whereas, Th-3,6Cz-Th-CH_3 with substituted methyl groups in 5-position of thiophene ring in the emission spectra is 356 nm, Th-3,6Cz-Th-$COCH_3$ with substituted acetyl groups in 5-position of thiophene ring in the emission spectra is 457 nm, Th-3,6Cz-Th-CHO with substituted formyl groups in 5-position of thiophene ring in the emission spectra is 475 nm.

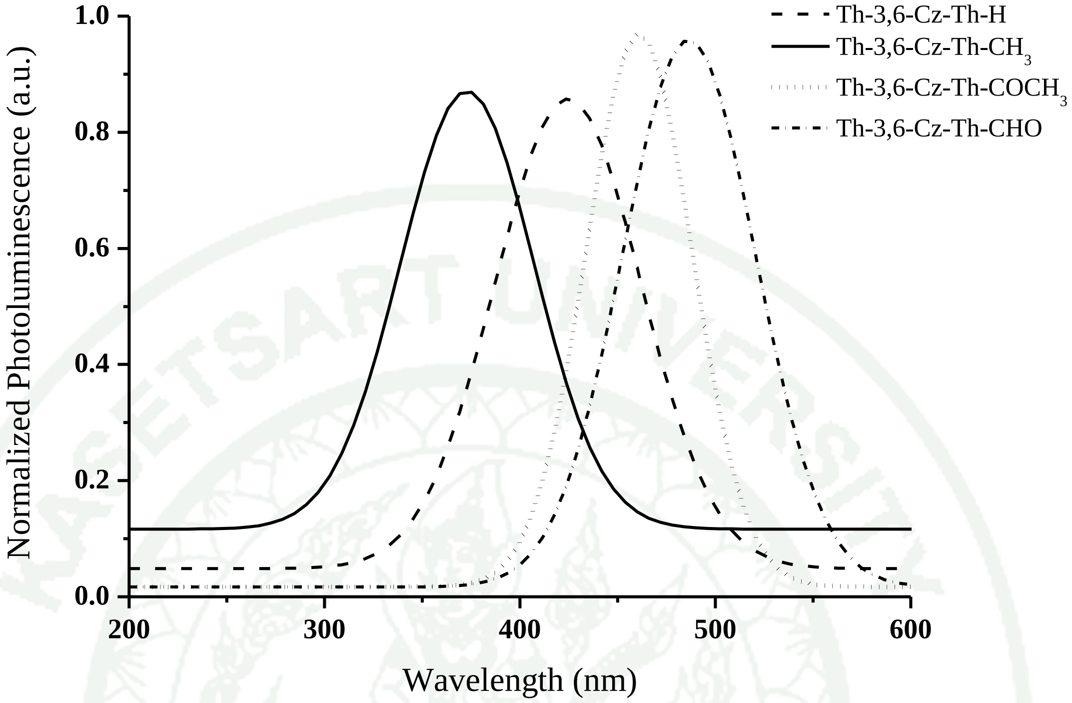

Figure 7 Emission spectra of Th-3,6Cz-Th-H, Th-3,6Cz-Th-CH_3, Th-3,6Cz-Th-$COCH_3$ and Th-3,6Cz-Th-CHO measured in dichloromethane solution.

Stokes shifts is the difference between of the absorption wavelength and emission wavelength. Stokes shifts of Th-3,6Cz-Th-H is 103 nm, whereas Th-3,6Cz-Th-CH_3 is 58 nm, Th-3,6Cz-Th-$COCH_3$ is 92 nm. Th-3,6Cz-Th-CHO is 82 nm. The results indicated that their main chain structures are rather rigid. However, the photophysical properties of Th-3,6Cz-Th-H, Th-3,6Cz-Th-CH_3, Th-3,6Cz-Th-$COCH_3$ are blue light emission, while Th-3,6Cz-Th-CHO exhibit as blue-green light emission. It is noteworthy that it can be used as new luminescence materials in the fabrication of OLED based full-color displays.

4. Fluorescence quantum yield

In optical spectroscopy, the quantum yield is the probability that a given quantum state is formed from the system initially prepared in some other quantum state. For example, a singlet to triplet transition state cross over to the triplet state. The fluorescence quantum yield gives the efficiency of the fluorescence process. It is defined as the number of photons emitted. The fluorescence quantum yields of the Th-3,6Cz-Th-H, Th-3,6Cz-Th-CH_3, Th-3,6Cz-Th-$COCH_3$, and Th-3,6Cz-Th-CHO compounds were measured in dichloromethane at room temperature by a relative method using quinine sulfate in sulfuric acid as a standard. The fluorescence quantum yields were calculated from the equation

$$\phi_s = \phi_r \frac{F_s}{F_r} \frac{A_r}{A_s} \left(\frac{n_r}{n_s} \right)^2$$

In the above equation, ø is the fluorescence quantum yield, *F* is the integration of the emission intensities, *n* is the index of reflection of the solution and *A* is the absorbance at the excitation wavelength, the subscripts '*r*' and 's' denote the reference and unknown samples, respectively. The fluorescence quantum yield (ø) were collected in Table 1. As shown in Table 1, the fluorescence quantum yield of the Th-3,6Cz-Th-H, Th-3,6Cz-Th-CH_3, Th-3,6Cz-Th-$COCH_3$, and Th-3,6Cz-Th-CHO are 0.25, 0.20, 0.57 and 0.79, respectively. The Th-3,6Cz-Th-$COCH_3$, and Th-3,6Cz-Th-CHO compounds showed high fluorescence quantum yields.

Quantum Chemical Calculations

1. Ground state and Excited state Structural Properties

The density function theory (DFT) method has been used for the purpose of conformation analysis. Bongini and Bottoni (1999) pointed that the DFT approach provides a good description of the conformation properties of oligomer and polythiophenes, which is agreement with the experimental evidence. Therefore, it will be useful to examine the structural parameters of Th-3,6Cz-Th-H, Th-3,6Cz-Th-CH_3, Th-3,6Cz-Th-$COCH_3$, and Th-3,6Cz-Th-CHO geometries based molecules with PBE0 functional method. Preliminary calculations all of the Th-3,6Cz-Th-H, Th-3,6Cz-Th-CH_3, Th-3,6Cz-Th-$COCH_3$, and Th-3,6Cz-Th-CHO structures were performed by using PBE0/6-31G(d) method for the ground state optimization (S_0) and TD-PBE0/6-31G(d) method for the first singlet excited state optimized geometries (S_1). The structural parameters in term of bond length were considered on backbone structure while the bond angle and torsion angle were studied only for thiophene-carbazole bridge position. Which it defined structures by excellent model systems that can be used to study conformation of all structures corresponding to the experimental results. In order to understand structural properties of the molecule, the ground state (S_0) and the first singlet excited state (S_1) geometries, bond length, bond angle and torsion angle, of Th-3,6Cz-Th-H, Th-3,6Cz-Th-CH_3, Th-3,6Cz-Th-$COCH_3$, and Th-3,6Cz-Th-CHO geometries were investigated.

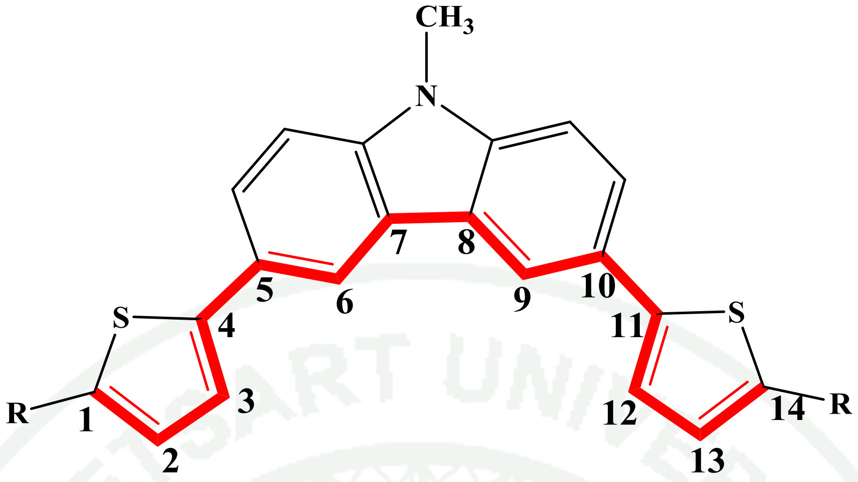

Figure 8 Schematic represents the bond number on the backbone structure of Th-3,6Cz-Th-R (R = -H, $-CH_3$, $-COCH_3$ and -CHO) molecule.

Table 2 Optimized bond lengths (in Å) of Th-3,6Cz-Th-R (R = H, CH_3, $COCH_3$ and CHO) obtained from PBE0/6-31G(d) and TD-PBE0/6-31G(d) methods

Bond length (Å)	R=H		R=CH_3		R=$COCH_3$		R=CHO	
	S_0	S_1	S_0	S_1	S_0	S_1	S_0	S_1
C1-C2	1.365	1.371	1.368	1.374	1.378	1.394	1.380	1.395
C2-C3	1.421	1.413	1.422	1.412	1.409	1.393	1.407	1.392
C3-C4	1.375	1.395	1.373	1.385	1.383	1.404	1.385	1.404
C4-C5	1.465	1.449	1.464	1.448	1.462	1.432	1.461	1.432
C5-C6	1.398	1.421	1.399	1.421	1.400	1.427	1.400	1.427
C6-C7	1.392	1.403	1.392	1.403	1.391	1.373	1.390	1.373
C7-C8	1.444	1.425	1.444	1.425	1.444	1.459	1.444	1.459
C8-C9	1.392	1.402	1.392	1.403	1.391	1.373	1.390	1.373
C9-C10	1.398	1.421	1.399	1.421	1.400	1.427	1.400	1.426
C10-C11	1.465	1.449	1.464	1.447	1.462	1.432	1.461	1.432
C11-C12	1.375	1.385	1.372	1.385	1.383	1.404	1.385	1.404
C12-C13	1.421	1.413	1.422	1.412	1.409	1.393	1.407	1.392
C13-C14	1.365	1.371	1.368	1.375	1.378	1.394	1.380	1.395
BLA	0.051	0.036	0.051	0.034	0.039	0.016	0.038	0.016

The C-C and C=C bond lengths of the optimized structures for the Th-3,6Cz-Th-H, Th-3,6Cz-Th-CH_3, Th-3,6Cz-Th-$COCH_3$, and Th-3,6Cz-Th-CHO are listed in Table 2. The bond length values were considered as the distance between the carbon atoms on the main chain structure. Unfortunately, from our knowledge, there is no X-ray structure of Th-3,6Cz-Th-H, Th-3,6Cz-Th-CH_3, Th-3,6Cz-Th-$COCH_3$, and Th-3,6Cz-Th-CHO structure available in literature. Therefore, this structural parameter with the quantum chemical calculations can be predicted the conformational analysis in this study. According to the results, in all cases the single bond lengths (C-C) became shorter and the double bond lengths (C=C) became larger, presented in Figure 8. The bond length was compared between Th-3,6Cz-Th-H, Th-3,6Cz-Th-CH_3, Th-3,6Cz-Th-$COCH_3$, and Th-3,6Cz-Th-CHO structure based on optimized geometries of the ground state (S_0) and the first singlet excited sate (S_1). The excitation to the S_1

state relaxes the bond alternation, the single bond lengths (see bond number C2-C3, C4-C5, C6-C7, C7-C8, C9-C10, C10-C11 and C12-C13) were calculated to be contracted in the S_1 state and the double bond lengths (see bond number C1-C2, C3-C4, C5-C6, C8-C9, C11-C12 and C13-C14) to be longer as shown in Table 2. Our calculations indicated that the bond length alterations by electron donating substitutions (methyl groups) are significant only for carbazole ring position, whereas the bond length alterations by electron withdrawing substitutions (acetyl and formyl groups) are significant for thiophene ring position.

Bond length changes in aromatic systems can also be described by bond length alternation (BLA). The BLA values for selected molecular fragment can be defined as the differences in the lengths between single bond and double bond between non-hydrogen atoms. The positive and negative sign of BLA indicated that the molecular unit has an aromatic and quinoid isomer, respectively. Thus, the BLA value can evaluated as following equations :

$$BLA = \left(\frac{\sum d_{single}}{n_{single}}\right) - \left(\frac{\sum d_{double}}{n_{double}}\right)$$

Where *d* symbols denote the bond determined of single bond and double bond distances on the backbone structure. As can be seen from data in Table 2, the Th-3,6Cz-Th-H, Th-3,6Cz-Th-CH_3, Th-3,6Cz-Th-$COCH_3$, and Th-3,6Cz-Th-CHO optimized geometries of the ground state (S_0) lead to increase of the BLA value, whereas the first singlet excited state (S_1) is decreased of the BLA value. From positive sign of BLA of four structures, it can be concluded that the main chain structures (C1-C14 atoms) are aromatic isomer.

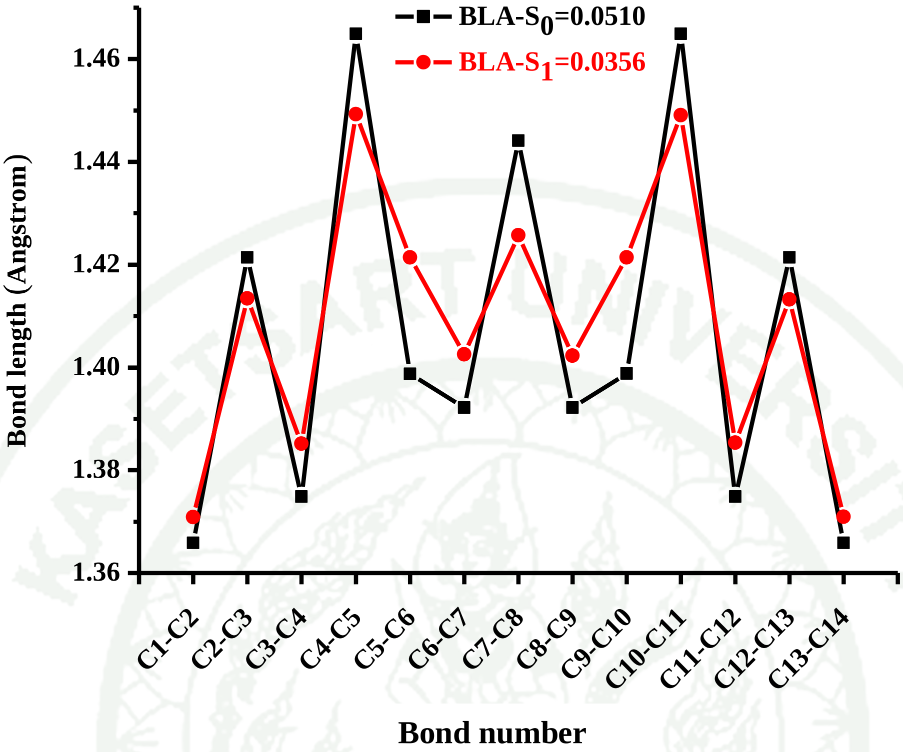

Figure 9 Optimized bond length and bond length alternation (BLA) of Th-3,6Cz-Th-H of the S_0 and S_1 geometries as obtained from PBE0/6-31G(d) and TD-PBE0/6-31G(d) methods, respectively.

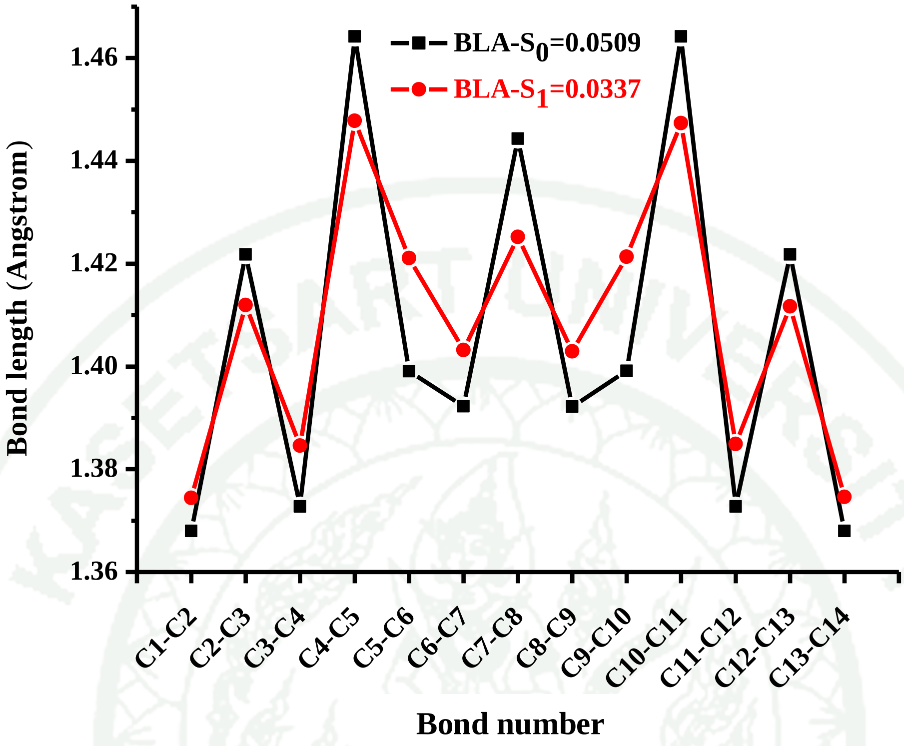

Figure 10 Optimized bond length and bond length alternation (BLA) of Th-3,6Cz-Th-CH_3 of the S_0 and S_1 geometries as obtained from PBE0/6-31G(d) and TD-PBE0/6-31G(d) methods, respectively.

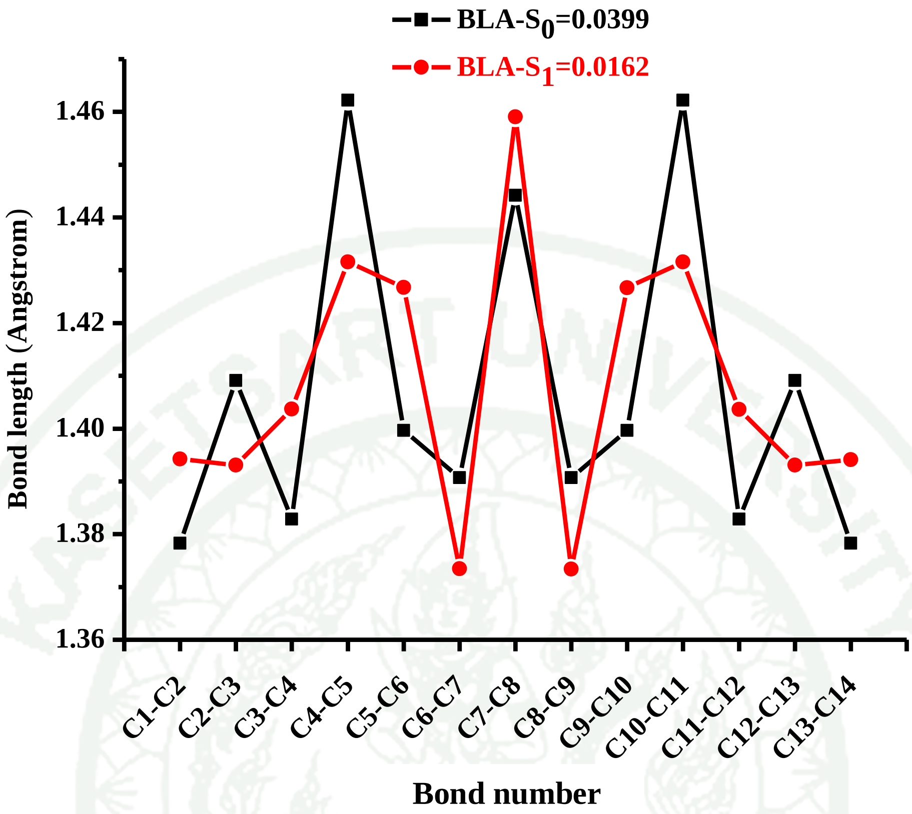

Figure 11 Optimized bond length and bond length alternation (BLA) of Th-3,6Cz-Th -COCH$_3$ of the S$_0$ and S$_1$ geometries as obtained from PBE0/6-31G(d) and TD-PBE0/6-31G(d) methods, respectively.

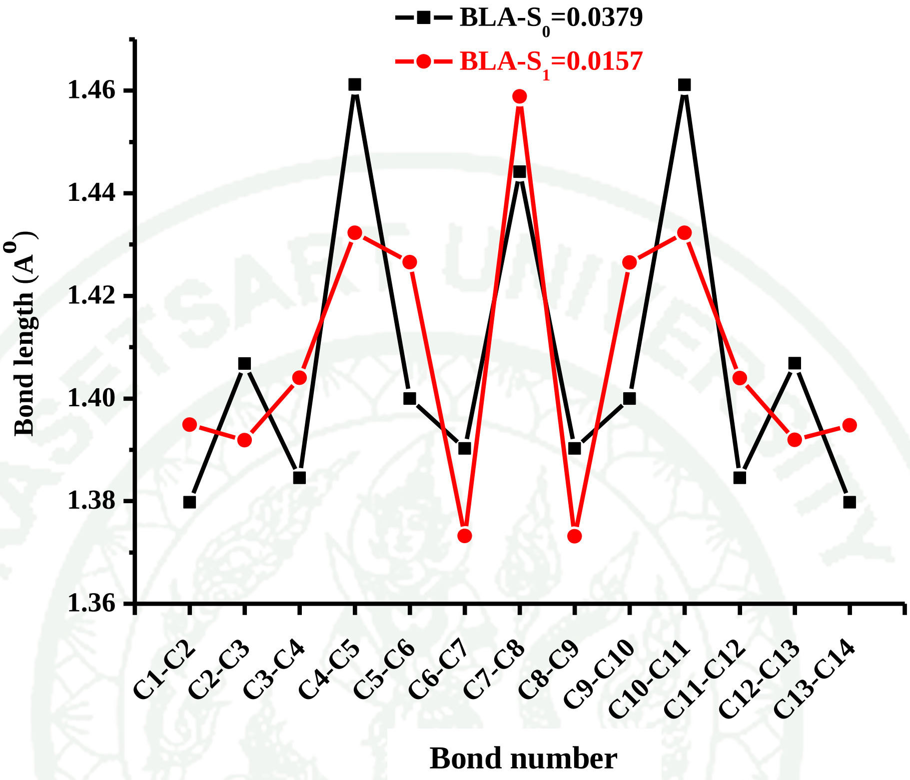

Figure 12 Optimized bond length and bond length alternation (BLA) of Th-3,6Cz-Th -CHO of the S_0 and S_1 geometries as obtained from PBE0/6-31G(d) and TD-PBE0/6-311G(d,p) methods, respectively.

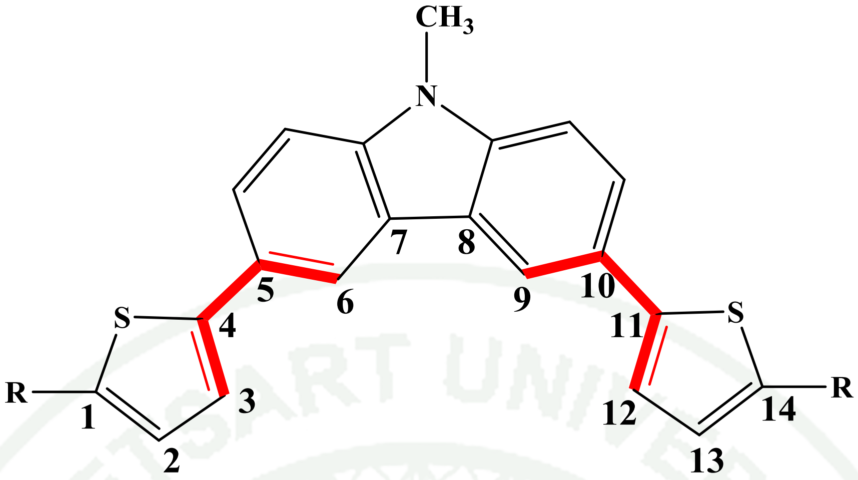

Figure 13 Schematic represent the bond numbering of Th-3,6Cz-Th-R (R = -H, $-CH_3$, $-COCH_3$ and -CHO) molecule.

Table 3 Optimized torsion angle (in degree) of Th-3,6Cz-Th-R (R = H, CH_3, $COCH_3$ and CHO) obtained from PBE0/6-31G(d) and TD-PBE0/6-31G(d) methods

Torsion angle (degree)	R=H		R=CH_3		R=$COCH_3$		R=CHO	
	S_0	S_1	S_0	S_1	S_0	S_1	S_0	S_1
∠C3-C4-C5-C6	27.9	17.9	26.9	15.9	25.1	0.3	24.7	0.2
∠C9-C10-C11-C12	27.8	17.8	26.8	16.2	25.9	0.3	24.5	0.3

The structural parameters of the torsion angles units of the Th-3,6Cz-Th-R (R = H, CH_3, $COCH_3$ and CHO) geometries between ground state (S_0) and first singlet excited state (S_1) geometries are summarized in Table 3. Investigation of the torsion angles of Th-3,6Cz-Th-R (R = H and CH_3) from S_0 geometries (around 27-28 degrees) slightly larger than S_1 geometries (around 16-18 degrees). The torsion angles of Th-3,6Cz-Th-R (R = $COCH_3$ and CHO) from S_0 geometries (around 25-26 degrees) larger than S_1 geometries (around 0.2-0.3 degrees). The ground-state structures of all molecules are non-planar with the torsion angle ∠C3-C4-C5-C6 and ∠C9-C10-C11-C12 (about ~25°) because of the steric repulsion. The excited state-torsion angles are more planar than the ground state geometries with torsional angles around 180 or 0 degree. The differences in the bond torsional angles between the ground and the lowest singlet excited state can be explained by considering the bond length changes. The results indicated that the bond length and torsion angle at S_1 geometries become closed to planar structure.

2. Electronic Properties

2.1 Absorption Properties

In order to understand the physical origin of optical transitions for the selected excitation energies, it is useful to examine the relevant (the highest) occupied and the lowest unoccupied molecular orbitals that play a dominant role. The PBE0/6-31G(d) method was used on the basis of the ground state optimized structures to compute vertical electron excitation energies, the highest occupied molecular orbital (HOMO) and the lowest unoccupied molecular orbital (LUMO), absorption wavelength and oscillator strength (*f*) of all structures were investigated in this work (Table 4). The calculated energies and absorption wavelength are compared with the experimental data in dichloromethane solution and quantum chemical calculation at TD-PBE0/6-311G(d,p) method optimized with PBE0/6-31G(d) level. The electronic transitions are described in detail below in term of the contribution to the excited state which the excitation take place.

The absorption wavelengths, oscillator strengths and excitation character of Th-Cz-Th, CH_3-Th-Cz-Th-CH_3, $COCH_3$-Th-Cz-Th-$COCH_3$, and CHO-Th-Cz-Th-CHO molecules are listed in Table 4, together with the experimental absorption spectra. The results shown that the absorption spectra of Th-3,6Cz-Th-H, Th-3,6Cz-Th-CH_3, Th-3,6Cz-Th-$COCH_3$, and Th-3,6Cz-Th-CHO (297.96, 334.16, 393.50 and 402.47 nm) are agreed well with the experimental spectra (302, 298, 365 and 393 nm) in dichloromethane solution. Moreover, the absorption wavelength in PCM model of Th-3,6Cz-Th-CH_3, Th-3,6Cz-Th-$COCH_3$, and Th-3,6Cz-Th-CHO in dichloromethane is slightly red-shift than that the experimental results.

Table 4 The lowest excitation energies in eV and oscillator strength (*f*) in solvent phase (in dichloromethane) using TD-PBE0/6-311G(d,p) method and absorption of experimental data in CH_2Cl_2 solution for the Th-3,6Cz-Th-R (R = H, CH_3, $COCH_3$ and CHO) geometries. H denoted HOMO and L is LUMO.

Electronic transitions	E_g (eV)	E_{ex} (nm)	*f*	Transition state	Experiment λ_{abs} (nm)
R=H					
$S_0 \rightarrow S_1$	3.61	342.76	0.0147	H→L (93%)	302 252
$S_0 \rightarrow S_2$	3.77	328.39	0.6536	H→L+1 (94%)	
$S_0 \rightarrow S_3$	4.16	297.96	0.6606	H-1→L (88%)	
$S_0 \rightarrow S_4$	4.24	292.01	0.1952	H→L+2 (96%)	
$S_0 \rightarrow S_5$	4.43	279.42	0.3487	H-1→L+1 (94%)	
R=CH_3					
$S_0 \rightarrow S_1$	3.55	348.97	0.0133	H→L (94%)	
$S_0 \rightarrow S_2$	3.71	334.16	0.8088	H→L+1 (95%)	
$S_0 \rightarrow S_3$	4.05	306.00	0.5525	H-1→L (90%)	298
$S_0 \rightarrow S_4$	4.18	296.50	0.2510	H→L+2 (97%)	
$S_0 \rightarrow S_5$	4.33	285.97	0.3225	H-1→L+1 (96%)	
R=$COCH_3$					
$S_0 \rightarrow S_1$	3.15	393.50	1.0077	H→L (97%)	
$S_0 \rightarrow S_2$	3.44	359.62	0.2130	H→L+1 (99%)	365
$S_0 \rightarrow S_3$	3.63	341.04	0.0022	H→L+2 (61%)	356
$S_0 \rightarrow S_4$	3.81	324.76	0.2205	H-1→L (64%)	318
$S_0 \rightarrow S_5$	3.84	322.57	0.2375	H-1→L+1 (68%)	

Table 4 (Continued)

Electronic transitions	E_g (eV)	E_{ex} (nm)	*f*	Transition state	Experiment λ_{abs} (nm)
R=CHO					
$S_0 \rightarrow S_1$	3.08	402.47	1.0083	H→L (97%)	
$S_0 \rightarrow S_2$	3.38	366.45	0.1915	H→L+1 (99%)	
$S_0 \rightarrow S_3$	3.60	343.84	0.0306	H-1→L (55%)	393
$S_0 \rightarrow S_4$	3.76	329.53	0.0934	H-5→L (32%)	250
$S_0 \rightarrow S_5$	3.76	329.06	0.0187	H-4→L (43%)	
$S_0 \rightarrow S_6$	3.78	327.57	0.2242	H-1→L +1 (58%)	

It is interesting to the excitation energies calculated by TDDFT corresponding to the absorption wavelength are underestimated when compared to the maximum wavelength from experimental results, as shown in Table 4. The calculated $S_0 \rightarrow S_1$ absorption energies, transition stated (H denoted HOMO and L is LUMO) and oscillator strength of the Th-3,6Cz-Th-R (R=$COCH_3$ and CHO) molecule and the corresponding experimental values are presented in Table 4. All $S_0 \rightarrow S_1$ transition consists of one-electron transitions mainly from HOMO to LUMO (H→L). The TDDFT results show that the absorption spectra of Th-3,6Cz-Th-H, Th-3,6Cz-Th-CH_3, Th-3,6Cz-Th-$COCH_3$, and Th-3,6Cz-Th-CHO (297.96, 334.16, 393.50 and 402.47 nm) is agreed well with the experimental spectra (302, 298, 365 and 393 nm) in dichloromethane solution which this absorption spectra in PCM model in dichloromethane solution is slightly differ from the experimental data.

The TDDFT excitation spectrum for the Th-3,6Cz-Th-H, Th-3,6Cz-Th-CH_3, Th-3,6Cz-Th-$COCH_3$, and Th-3,6Cz-Th-CHO compounds are compared to the experimental absorption spectra as shown in Figure 14, 15, 16 and 17. The theoretical absorption spectrum of the Th-3,6Cz-Th-H, Th-3,6Cz-Th-CH_3, Th-3,6Cz-Th-$COCH_3$, and Th-3,6Cz-Th-CHO compound consists of closely peaks with large oscillator strength, the highest oscillator strength (π–π* transition) of all states calculated by TD-PBE0/6-311G(d,p) method which are compared to the experimental absorption spectra in Figure 14, 15, 16 and 17. This is in good agreement with the experimental measurements. All of these states are assigned to the π→π* transition corresponding to the transition from HOMO to LUMO, HOMO→L+1 and H-1→L+1 transitions. The introduction of $COCH_3$ and CHO groups on the 9-octyl-3,6-di(thiophen-2-yl)-Carbazole to bathochromic shift of the absorption wavelengths of carbazoles derivatives.

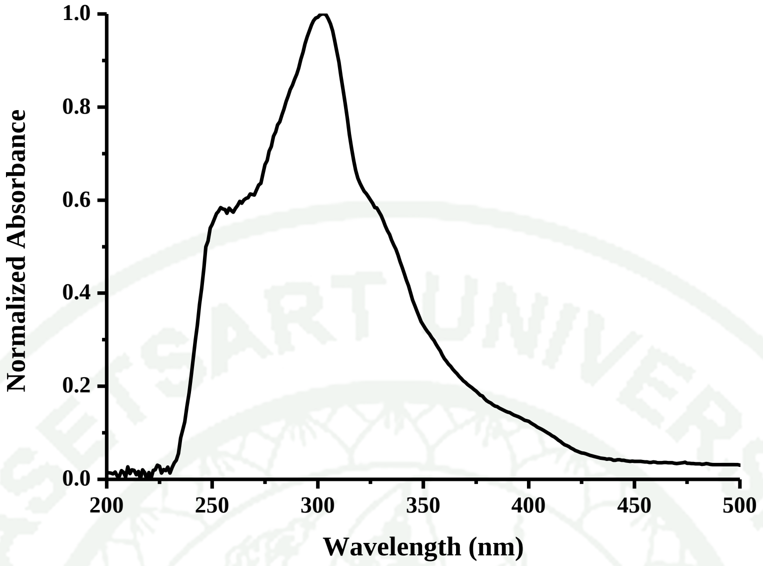

(a)

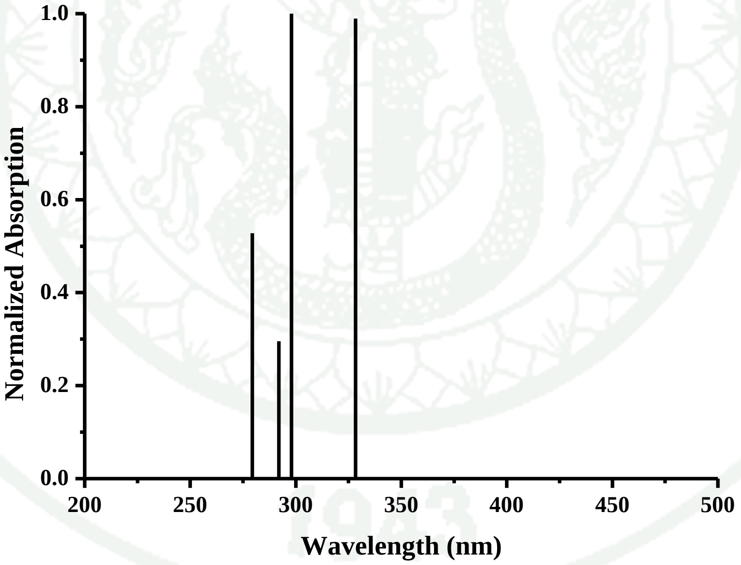

(b)

Figure 14 Absorption spectra of Th-3,6Cz-Th-H obtained from the experimental in CH_2Cl_2 solution (a) and calculated using TD-PBE0/6-311G(d,p) in PCM model (b).

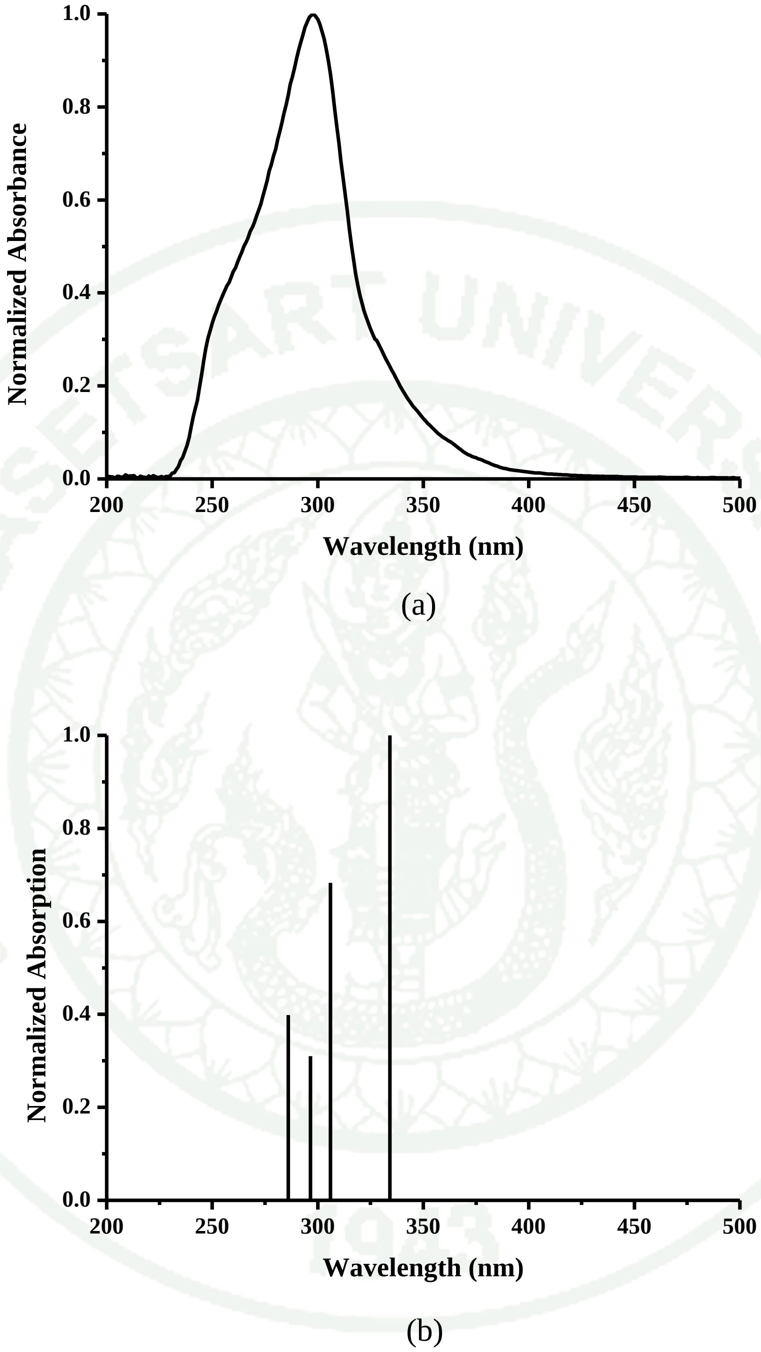

(a)

(b)

Figure 15 Absorption spectra of Th-3,6Cz-Th-CH_3 obtained from the experimental in CH_2Cl_2 solution (a) and calculated using TD-PBE0/6-311G(d,p) in PCM model (b).

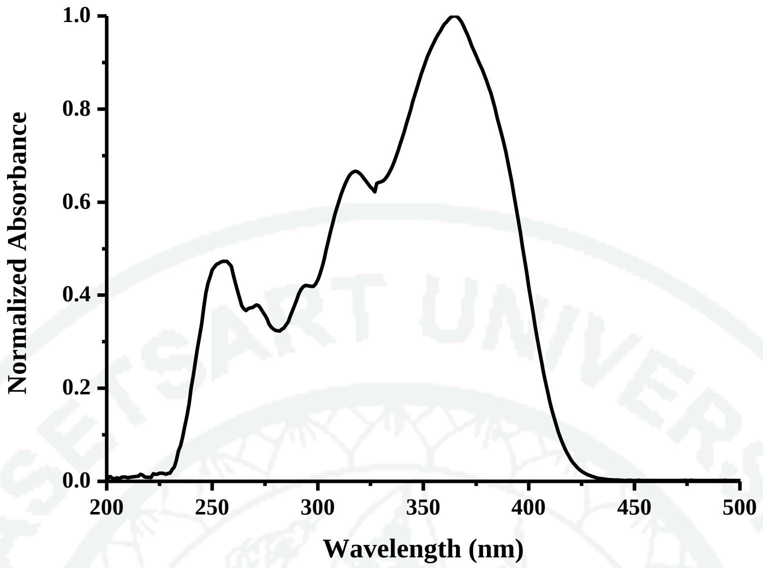

(a)

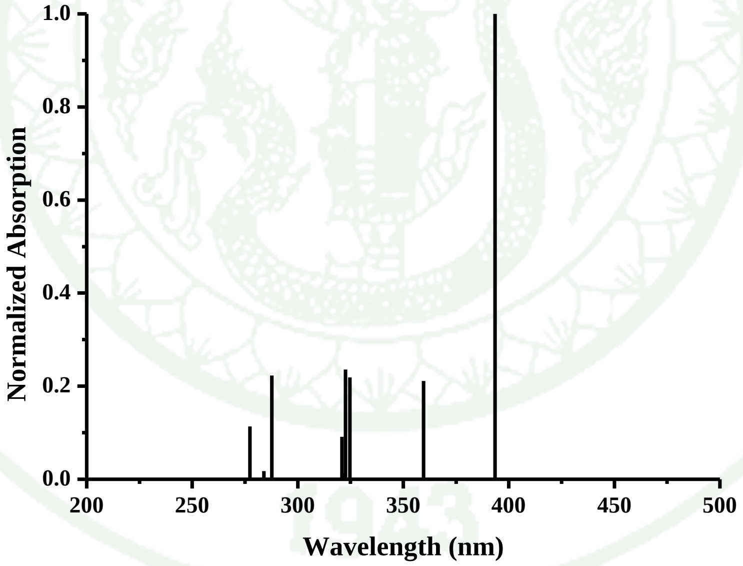

(b)

Figure 16 Absorption spectra of Th-3,6Cz-Th-$COCH_3$ obtained from experimental in CH_2Cl_2 solution (a) and calculated using TD-PBE0/6-311G(d,p) in PCM model (b).

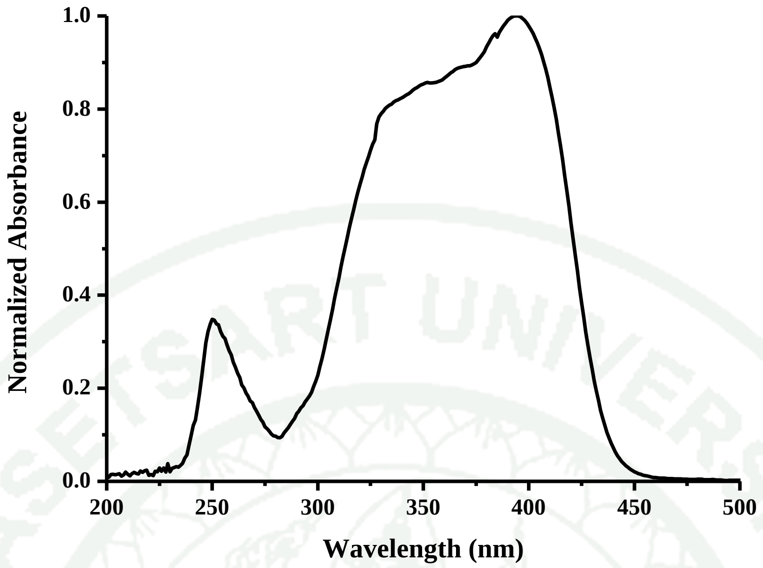

(a)

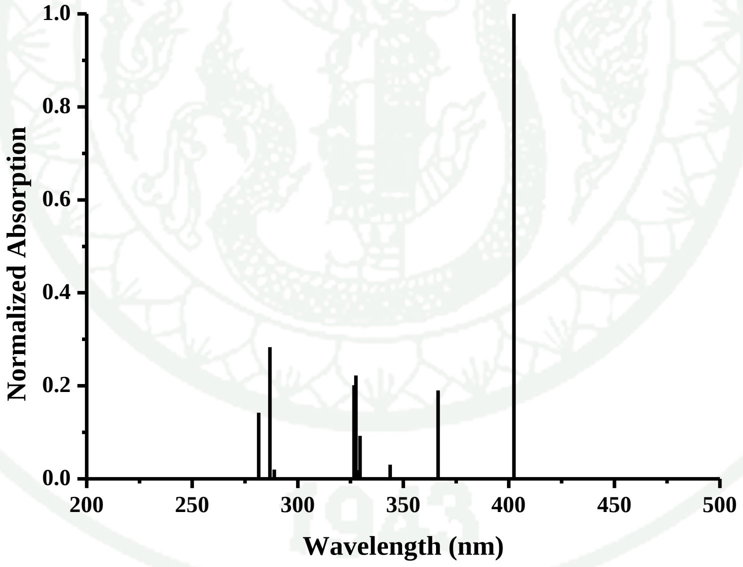

(b)

Figure 17 Absorption spectra of Th-3,6Cz-Th-CHO obtained from the experimental in CH_2Cl_2 solution (a) and calculated using TD-PBE0/6-311G(d,p) in PCM model (b).

For the lowest excitation energy, the electron is excited from the highest occupied molecular orbitals (HOMO) to the lowest unoccupied molecular orbital (LUMO). This transition is $\pi \rightarrow \pi^*$ character arising exclusively from $S_0 \rightarrow S_1$ electronic transition mainly composed by HOMO→LUMO transition. However, the orbital presentation of the next transitions is different with respect to the substation. In the HOMO and next HOMO, double bonds form bonding orbitals, and the single bonds are antibonding. In the LUMO, double bonds are antibonding and the single bonds are bonding on the backbone structure.

The molecular orbitals relevant for the Th-3,6Cz-Th-H, Th-3,6Cz-Th-CH_3, Th-3,6Cz-Th-$COCH_3$, and Th-3,6Cz-Th-CHO molecules presented in Figure 18. In the HOMO of Th-3,6Cz-Th-H and Th-3,6Cz-Th-CH_3 molecules, the electrons are localized on the backbone structure. The LUMO contains localization on the carbazole structure.

In the HOMO of Th-3,6Cz-Th-$COCH_3$, and Th-3,6Cz-Th-CHO molecules, the electrons are localized on the backbone structure. The LUMO contains localization on the thiophene ring and substitutents structure. The results show that Th-3,6Cz-Th-$COCH_3$, and Th-3,6Cz-Th-CHO molecules, which are electron withdrawing group allowed the electron delocalized on the thiophene and substituents structure.

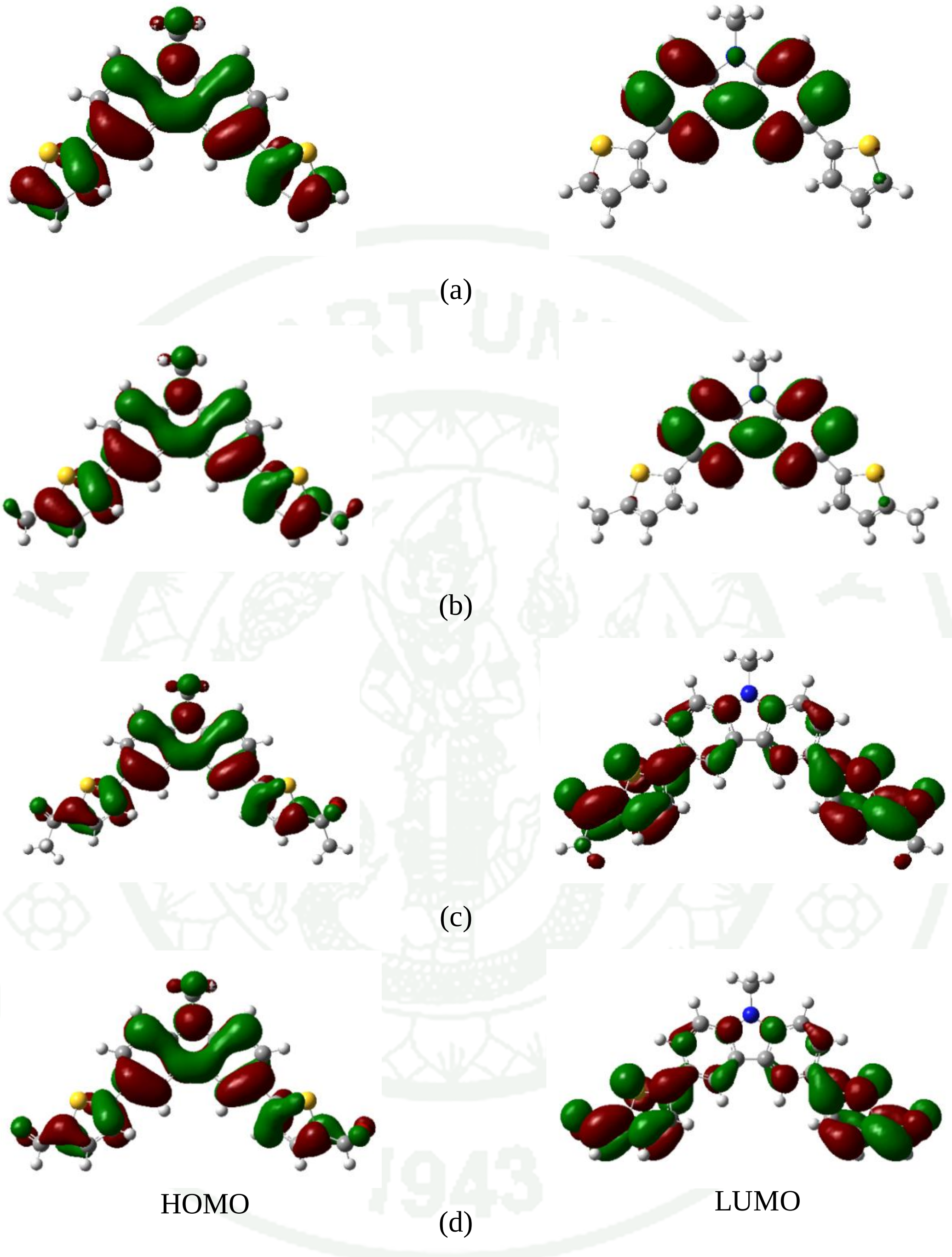

Figure 18 Structures of molecular orbitals for (a) Th-3,6Cz-Th-H, (b) Th-3,6Cz-Th-CH_3, (c) Th-3,6Cz-Th-$COCH_3$ and (d) Th-3,6Cz-Th-CHO molecules.

2.2 Emission Properties

The emission calculations are performed by vertical de-excitation of the compounds of Th-3,6Cz-Th-H, Th-3,6Cz-Th-CH_3, Th-3,6Cz-Th-$COCH_3$, and Th-3,6Cz-Th-CHO molecules with the PBE0/6-31G(d) method in their first singlet excited state, followed by using the resulting geometries to perform TD-DFT calculations employing the PBE0/6-311G(d,p) method from the singlet ground state. Table 6 indicated the calculated fluorescence of Th-3,6Cz-Th-H and Th-3,6Cz-Th-CH_3 molecule 348.78 and 356.57 nm. The luminescence peak at 405 and 336 nm of experimental spectra is close to the Th-3,6Cz-Th-H and Th-3,6Cz-Th-CH_3 geometries using TD-DFT method (348.78 and 356.57 nm). The calculated fluorescence of Th-3,6Cz-Th-$COCH_3$ and Th-3,6Cz-Th-CHO molecules are 444.06 and 449.57 nm for S_1 with the largest oscillator strength arising from HOMO→LUMO corresponding to π-π*excitation and it is close to the experimental results of 457 and 475 nm.

Table 5 The emission energies in eV and oscillator strength (*f*) in solvent phase (in dichloromethane) using TD-PBE0/6-311G(d,p) method and emission of experimental data in CH_2Cl_2 solution for the Th-3,6Cz-Th-R (R = H, CH_3, $COCH_3$ and CHO) geometries. H denoted HOMO and L is LUMO.

Electronic transitions	E_g (eV)	E_{ex} (nm)	*f*	Transition state	Experiment λ_{abs} (nm)
R=H					
$S_1 \rightarrow S_0$	3.33	371.00	0.0184	H→L (95%)	405
$S_2 \rightarrow S_0$	3.55	348.78	0.6678	H→L+1 (94%)	
R=CH_3					
$S_1 \rightarrow S_0$	3.26	380.00	0.0163	H→L (95%)	356
$S_2 \rightarrow S_0$	3.47	356.57	0.8277	H→L+1 (95%)	

Table 5 (Continued)

Electronic transitions	E_g (eV)	E_{ex} (nm)	*f*	Transition state	Experiment λ_{abs} (nm)
R=COCH$_3$					
$S_1 \rightarrow S_0$	2.79	444.06	1.2205	H→L (98%)	457
$S_2 \rightarrow S_0$	3.18	389.00	0.1935	H→L+1 (98%)	
R=CHO					
$S_1 \rightarrow S_0$	2.75	449.57	1.2196	H→L (98%)	475
$S_2 \rightarrow S_0$	3.15	393.22	0.1615	H→L+1 (96%)	

Table 6 The wavelength of emission energies, stokes shifts and radiative lifetime (τ) using TD-PBE0/6-311G(d,p) method and experimental data in CH_2Cl_2 solution for the Th-3,6Cz-Th-H, Th-3,6Cz-Th-CH_3, Th-3,6Cz-Th-$COCH_3$, and Th-3,6Cz-Th-CHO.

Compound	E_{Flu} (eV)		Stokes shifts		τ (s)
	Cal.	Expt.	Cal.	Expt.	
Th-3,6Cz-Th-H	3.33	3.06	0.83	1.04	$1.13\text{x}10^{-7}$
Th-3,6Cz-Th-CH_3	3.26	3.48	0.45	0.68	$1.33\text{x}10^{-7}$
Th-3,6Cz-Th-$COCH_3$	2.79	2.71	0.36	0.68	$2.43\text{x}10^{-9}$
Th-3,6Cz-Th-CHO	2.75	2.61	0.33	0.55	$1.82\text{x}10^{-9}$

The differences between frequency or wavelength of the emitted and absorbed light is called the Stokes shift. Evaluation of the Stokes shift is the differences $\Delta E = E_{abs}\text{-}E_{flu}$. The TD-PBE0/6-311G(d,p) and experimental values exhibit Stokes shift of Th-3,6Cz-Th-CHO are lower than Th-3,6Cz-Th-H, Th-3,6Cz-Th-CH_3 and Th-3,6Cz-Th-$COCH_3$. This result demonstrates that the Th-3,6Cz-Th-CHO structure is more relaxed than those of Th-3,6Cz-Th-H, Th-3,6Cz-Th-CH_3 and Th-3,6Cz-Th-$COCH_3$ upon excitation and the result corresponding with the radiative lifetime.

CONCLUSION AND RECOMMENDATION

Conclusion

The syntheses of 9-octyl-3,6-di(thiophene-2-yl)-carbazole derivatives have been carried out. All of these compounds were synthesized via Suzuki reaction. These compounds were confirmed by ^{1}H-NMR, UV-Vis and fluorescence measurements. The absorption behavior of Th-3,6Cz-Th-H (302 nm), Th-3,6Cz-Th-CH_3 (298 nm), Th-3,6Cz-Th-$COCH_3$ (365 nm) and Th-3,6Cz-Th-CHO (393 nm) and optical band gap energies with the absorption onset are 4.10, 4.16, 3.39 and 3.16 eV, respectively. The electron-withdrawing acetyl and formyl groups on the substituent thiophene moiety can further give red shifts in the absorption and emission spectra. The photophysical properties of Th-3,6Cz-Th-H, Th-3,6Cz-Th-CH_3 and Th-3,6Cz-Th-$COCH_3$ exhibited as blue light emission, while Th-3,6Cz-Th-CHO exhibited as blue-green light emission. It is noteworthy that can be used as new luminescence materials in the fabrication of OLED-based full-color displays.

The experimental data was confirmed with results obtained from quantum chemical calculations. Therefore, the structural conformations (S_0 and S_1) and electronic properties of Th-3,6Cz-Th-H, Th-3,6Cz-Th-CH_3, Th-3,6Cz-Th-$COCH_3$ and Th-3,6Cz-Th-CHO geometries were performed. The PBE0/6-31G(d) method was used for the systematic theoretical investigation of the conformation analysis. The substitutions of the thiophene unit by electron-withdrawing (-$COCH_3$, -CHO) and electron-donating (methyl) group were considered. Most of the derivative of Th-3,6Cz-Th-H molecule exhibit planar structures at excitation state. The excited state-torsion angles are more planar than the ground state geometries. The absorption properties and fluorescence wavelength were investigated using TD-PBE0/6-311G(d,p) method. The obtained results of the electronic transition of structural geometries indicate that calculated UV-vis absorption spectra related with the experimental data.

Recommendation

1. For experimental section, temperature must be controlled during the experiment. In addition, the time of reflux should be longer if the amount of reactants increase.

2. Thermal analysis is recommended for measure thermal properties of compound.

LITERATURE CITED

Becke, A.D. 1993. Density-functional thermochemistry. III. The role of exact exchange. **J. Chem. Phys.** 98(7):5648-5652.

Belletête, M., M. Bédard, M. Leclerc and G. Durocher. 2004. Absorption and emission properties of carbazole-based dyads studied from experimental and theoretical investigations. **Synthetic. Met.** 146(1): 99-108.

Belletête, M., M. Bédard, M. Leclerc and G. Durocher. 2004. Ground and excited state properties of carbazole-based dyads: Correlation with their respective absorption and fluorescence spectra. **J. Mol. Struc-THEOCHEM.** 679(1-2): 9-15.

Belloni, M., B. M. Kariuki, M. Manickam, J. Wilkie and J. A. Preece. 2005. Design of potentially photorefractive liquid crystalline materials: Derivatives of 3,6-disubstituted carbazole. **Cryst. Growth. Des.** 5(4): 1443-1450.

Blondin, P., J. Bouchard, S. Beaupré, M. Belletête, G. Durocher and M. Leclerc. 2000. Molecular design and characterization of chromic polyfluorene derivatives. **Macromolecules.** 33(16): 5874-5879.

Brunner, K., A. Van Dijken, H. Börner, J. J. A. M. Bastiaansen, N. M. M. Kiggen and B. M. W. Langeveld. 2004. Carbazole compounds as host materials for triplet emitters in organic light-emitting diodes: Tuning the HOMO level without influencing the triplet energy in small molecules. **J. Am. Chem. Soc.** 126(19): 6035-6042.

Cao, Y., I.D. Parker, G. Yu, C. Zhang and A.J. Heeger. 1999. Improved quantum efficiency for electroluminescence in semiconducting polymers. **Nature.** 397(6718):414-415.

Cleave, V., G. Yahioglu, P.L. Barny, R.H. Friend and N. Tessler. 1999. Harvesting singlet and triplet energy in polymer LEDs. **Adv. Mater.** 11(4):285-288.

Corral, C., D. Sempere-Torres, M. Revilla and M. Berenguer. 2000. A semi-distributed hydrological model using rainfall estimates by radar. Application to Mediterranean basins. **Phys. Chem. Earth, Part B: Hydrology, Oceans and Atmosphere** 25(10-12):1133-1136.

Di Césare, N., M. Belletête, G. Durocher and M. Leclerc. 1997. Towards a theoretical design of thermochromic polythiophenes. **Chem. Phys. Lett.** 275(5-6): 533-539.

Dimitrakopoulos, C. D. and P. R. L. Malenfant 2002. Organic thin film transistors for large area electronics. **Adv. Mater.** 14(2): 99-117.

Dobarro, A., D. Velasco, V. V. Arnim and H. Finkelmann. 1997. Synthesis of symmetric and asymmetric carbazolyl monomers and their siloxane polymers. Effect of the 2,3,6,7,9-substitution in the carbazole unit on its mesomorphic behaviour. **Macromol. Chem. Phys.** 198(8): 2563-2581.

Doskocz, J., M. Doskocz, S. Roszak, J. Soloducho and J. Leszczynski. 2006. Theoretical studies of symmetric five-membered heterocycle derivatives of carbazole and fluorene: Precursors of conducting polymers. **J. Phys. Chem. A.** 110(51): 13989-13994.

Feng, G. L., W. Y. Lai, S. J. Ji and W. Huang. 2006. Synthesis of novel star-shaped carbazole-functionalized triazatruxenes. **Tetrahedron. Lett.** 47(39): 7089-7092.

Fong Wallace, H. H., C. H. Choy, K. N. Hui and Y. J. Liang. 2006. Organic light-emitting diodes based on a cohost electron transporting composite. **Appl. Phys. Lett.** 88(11).

Gong, Z. and J. B. Lagowski. 2008. Theoretical study of the structures and electronic properties of the dimers of fluorene and carbazole and their derivatives. **J. Mol. Struc-THEOCHEM.** 866(1-3): 27-33.

Grigalevicius, S. 2006. 3,6(2,7),9-Substituted carbazoles as electroactive amorphous materials for optoelectronics. **Synthetic. Met.** 156(1): 1-12.

Grozema, F.C. and J.M. Warman. 2005. Highly mobile electrons and holes on polyfluorene chains formed by charge scavenging in pulse-irradiated trans-decalin solutions. **Radiat. Phys. Chem.** 74(3-4):234-238.

Huang, Y.M., J.W.Y. Lam, K.K.L. Cheuk, W. Ge and B.Z. Tang. 2001. The role of the phenyl and biphenyl chromophores in the blue luminescent liquid crystalline polyacetylenes. **Mat. Sci. Eng. B-solid.** 85(2-3):242-246.

Hutchison, G.R., M.A. Ratner, and T.J. Marks. 2002. Accurate prediction of band gaps in neutral heterocyclic conjugated polymers. **J. Phys. Chem. A.** 106:10596-10605.

Iraqi, A., D. F. Pickup and H. Yi. 2006. Effects of methyl substitution of poly(9-alkyl-9H-carbazole-2,7-diyl)s at the 3,6-positions on their physical properties. **Chem. Mater.** 18(4): 1007-1015.

Iraqi, A. and I. Wataru. 2004. 3,6-Linked 9-alkyl-9H-carbazole main-chain polymers: Preparation and properties. **J. Polym. Sci. Pol. Chem.** 42(23): 6041-6051.

Jacquemin, D. and E.A. Perp̀te. 2006. Ab initio calculations of the colour of closed-ring diarylethenes: TD-DFT estimates for molecular switches. **Chem. Phys. Lett.** 429(1-3):147-152.

Katz, H. E. 2004. Recent advances in semiconductor performance and printing processes for organic transistor-based electronics. **Chem. Mater.** 16(23): 4748-4756.

Lamansky, S., R. C. Kwong, M. Nugent, P. I. Djurovich and M. E. Thompson 2001. Molecularly doped polymer light emitting diodes utilizing phosphorescent Pt(II) and Ir(III) dopants. **Org. Electron.** 2(1): 53-62.

Law, K. Y. 1993. Organic photoconductive materials: Recent trends and developments. **Chem. Rev.** 93(1): 449-486.

Leclerc, M., G. Dufresne, P. Blondin, J. Bouchard, M. Belletête and G. Durocher. 2001. Molecular design of chromic functionalized conjugated polymers. **Synthetic. Met.** 119(1-3): 45-48.

Lee, C., W. Yang and R.G. Parr. 1988. Development of the Colle-Salvetti correlation-energy formula into a functional of the electron density. **Phys. Rev. B.** 37(2):785.

Lee, S. J., J. S. Park, K. Yoon, Y. Kim, S. Jin, S. K. Kang, Y. Gal, S. Kang, J. Y. Lee, J. Kang,. 2008. High-efficiency deep-blue light-emitting diodes based on phenylquinoline/carbazole-based compounds. **Adv. Funct. Mater.** 18(24): 3922-3930.

Link, J. T., S. Raghavan, M. Gallant, S. J. Danishefsky, T. C. Chou and L. M. Ballas. 1996. Staurosporine and ent-staurosporine: The first total syntheses, prospects for a regioselective approach, and activity profiles. **J. Am. Chem. Soc.** 118(12): 2825-2842.

Malinsky, J.E., G.E. Jabbour, S.E. Shaheen, J.D. Anderson, A.G. Richter, T.J. Marks, N.R. Armstrong, B. Kippelen, P. Dutta and N. Peyghambarian. 1999. Self-assembly processes for organic LED electrode passivation and charge injection balance. **Adv. Mater.** 11(3):227-231.

Meeto, W., S. Suramitr, S. Vannarat and S. Hannongbua. 2008. Structural and electronic properties of poly(fluorene-vinylene) copolymer and its derivatives: Time-dependent density functional theory investigation. **Chem. Phys.** 349(1-3):1-8.

Mitschke, U. and P. Bauerle 2000. The electroluminescence of organic materials. **J. Mater. Chem.** 10(7): 1471-1507.

Morin, J. F. and M. Leclerc. 2002. 2,7-Carbazole-based conjugated polymers for blue, green, and red light emission. **Macromolecules.** 35(22): 8413-8417.

Morin, J. F., M. Leclere, D. Adès and A. Siove 2005. Polycarbazoles: 25 years of progress. **Macromol. Rapid. Comm.** 26(10): 761-778.

Ogundare, F.O. and M.L. Chithambo. 2008. The influence of optical bleaching on lifetimes and luminescence intensity in the slow component of optically stimulated luminescence of natural quartz from Nigeria. **J. Lumin.** 128(10):1561-1569.

Ostroverkhova, O. and W. E. Moerner 2004. Organic photorefractives: Mechanisms, materials, and applications. **Chem. Rev.** 104(7): 3267-3314.

Paliulis, O., J. Ostrauskaite, V. Gaidelis, V. Jankauskas and P. Strohriegl. 2003. Synthesis of conjugated carbazole trimers and pentamers by suzuki coupling. **Macromol. Chem. Phys.** 204(14): 1706-1712.

Pan, J. H., H. L. Chiu and B. C. Wang. 2005. Theoretical investigation of carbazole derivatives as hole-transporting materials in OLEDs. **J. Mole. Struc-THEOCHEM.** 725(1-3): 89-95.

Pickup, D. F., H. Yi, H. Kun, A. Iraqi, M. Stevenson and D. G. Lidzey. 2009. Alternating 2,7- and 3,6-linked carbazole copolymers as wide band gap energy transfer donors. **Thin. Solid. Films.** 517(9): 2840-2844.

Poolmee, P., M. Ehara, S. Hannongbua and H. Nakatsuji. 2005. SAC-CI theoretical investigation on electronic structure of fluorene-thiophene oligomers. **Polymer.** 46(17):6474-6481.

Promarak, V. and S. Ruchirawat. 2007. Synthesis and properties of N-carbazole end-capped conjugated molecules. **Tetrahedron.** 63(7): 1602-1609.

Romero, D. B., M. Schaer, M. Leclerc, D. Adès, A. Siove and L. Zuppiroli. 1996. The role of carbazole in organic light-emitting devices. **Synthetic. Met.** 80(3): 271-277.

Sheats, J.R., Y.-L. Chang, D.B. Roitman and A. Stocking. 1999. Chemical aspects of polymeric electroluminescent devices. **Accounts. Chem. Res.** 32(3):193-200.

Shi, H. p., Y. Cheng, W. j. Jing, J. B. Chao, L. Fang, X. Dong and C. Dong. 2010. Experimental and theoretical study of a new carbazole derivative having terminal benzimidazole rings. **Spectrochim. Acta. A.** 75(2): 525-532.

Shirota, Y., M. Kinoshita, T. Noda, K. Okumoto and T. Ohara. 2000. A novel class of emitting amorphous molecular materials as bipolar radical formants: 2-{4-[Bis(4-methylphenyl)amino]phenyl}-5-(dimesitylboryl)thiophene and 2-{4-[Bis(9,9-dimethylfluorenyl)amino]phenyl}-5-(dimesitylboryl)thiophene. **J. Am. Chem. Soc.** 122(44): 11021-11022.

Shirota, Y., Y. Kuwabara, H. Inada, T. Wakimoto, H. Nakada, Y. Yonemoto, S. Kawami and K. Imai. 1994. Multilayered organic electroluminescent device using a novel starburst molecule, 4,4',4]-tris(3-methylphenylphenylamino) triphenylamine, as a hole transport material. **Appl. Phys. Lett.** 65(7): 807-809.

Shirota, Y., K. Okumoto and H. Inada. 2000. Thermally stable organic light-emitting diodes using new families of hole-transporting amorphous molecular materials. **Synthetic. Met.** 111: 387-391.

Suramitr, S., S. Hannongbua and P. Wolschann. 2007. Conformational analysis and electronic transition of carbazole-based oligomers as explained by density functional theory. **J. Mol. Struc-THEOCHEM** 807(1-3): 109-119.

Tang, C. W. and S. A. Vanslyke. 1987. Organic electroluminescent diodes. **Appl. Phys. Lett.** 51(12): 913-915.

Yamashita, Y., N. Fujii, C. Murakata, T. Ashizawa, M. Okabe and H. Nakano 1992. Induction of mammalian DNA topoisomerase I mediated DNA cleavage by antitumor indolocarbazole derivatives. **Biochemistry-US.** 31(48): 12069-12075.

Yang, M. J. and T. Tsutsui 2000. Use of poly(9-vinylcarbazole) as host material for iridium complexes in high-efficiency organic light-emitting devices. **Jpn. J. Appl. Phys.** 39(8 A).

Zhang, Y., T. Wada and H. Sasabe. 1998. Carbazole photorefractive materials. **J. Mater. Chem.** 8(4): 809-828.

Zhang, Y., T. Wada, L. Wang and H. Sasabe. 1997. Amorphous conjugated carbazole trimers for photorefractive materials. **Chem. Mater.** 9(12): 2798-2804.

Zhu, M., T. Cui and K. Varahramyan. 2004. Experimental and theoretical investigation of MEH-PPV based Schottky diodes. **Microelectron. Eng.** 75(3):269-274.

APPENDICES

Appendix A

Supporting information

1. 3,6-dibromo-9H-carbazole (A2)

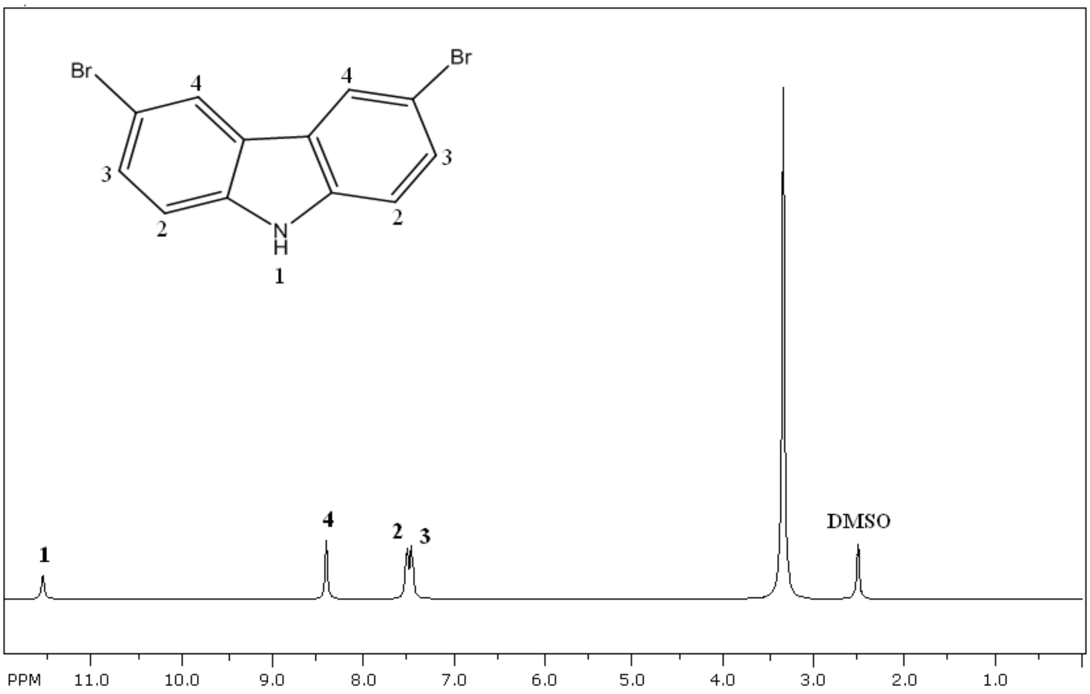

Appendix Figure A1 ^{1}H-NMR spectrum of 3,6-dibromo-9H-carbazole.

2. 3,6-Dibromo-9-octyl-carbazole (A3)

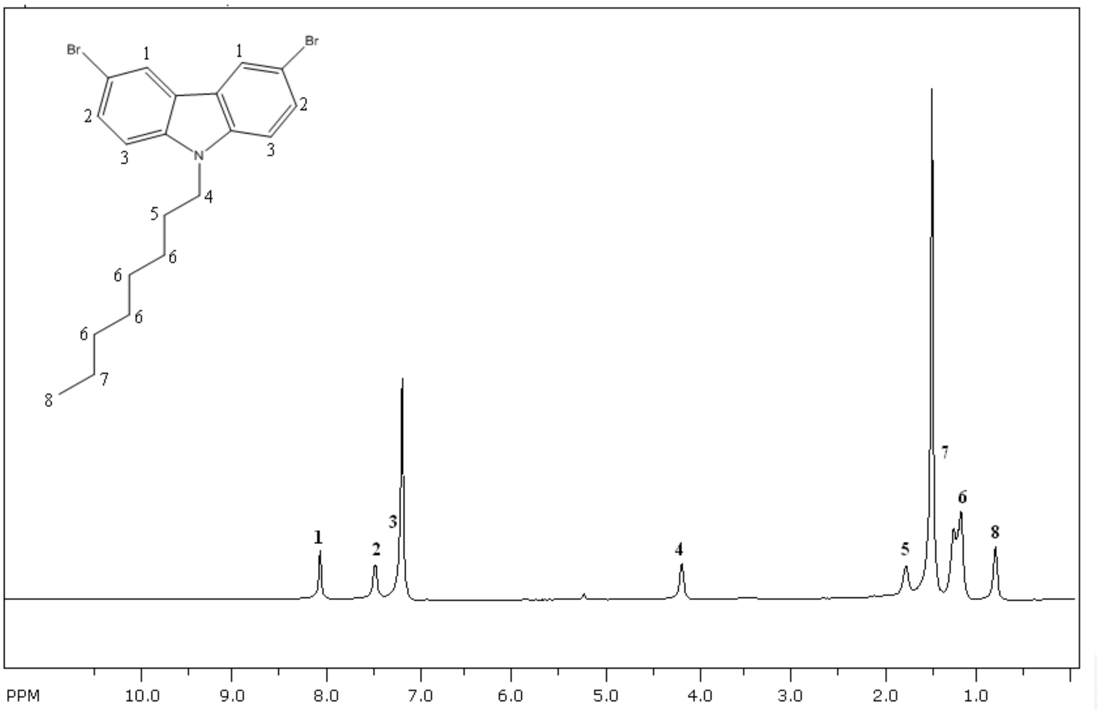

Appendix Figure A2 ^{1}H-NMR spectrum of 3,6-Dibromo-9-octyl-carbazole.

3. 9-octyl-3,6-di(thiophen-2-yl)-carbazole

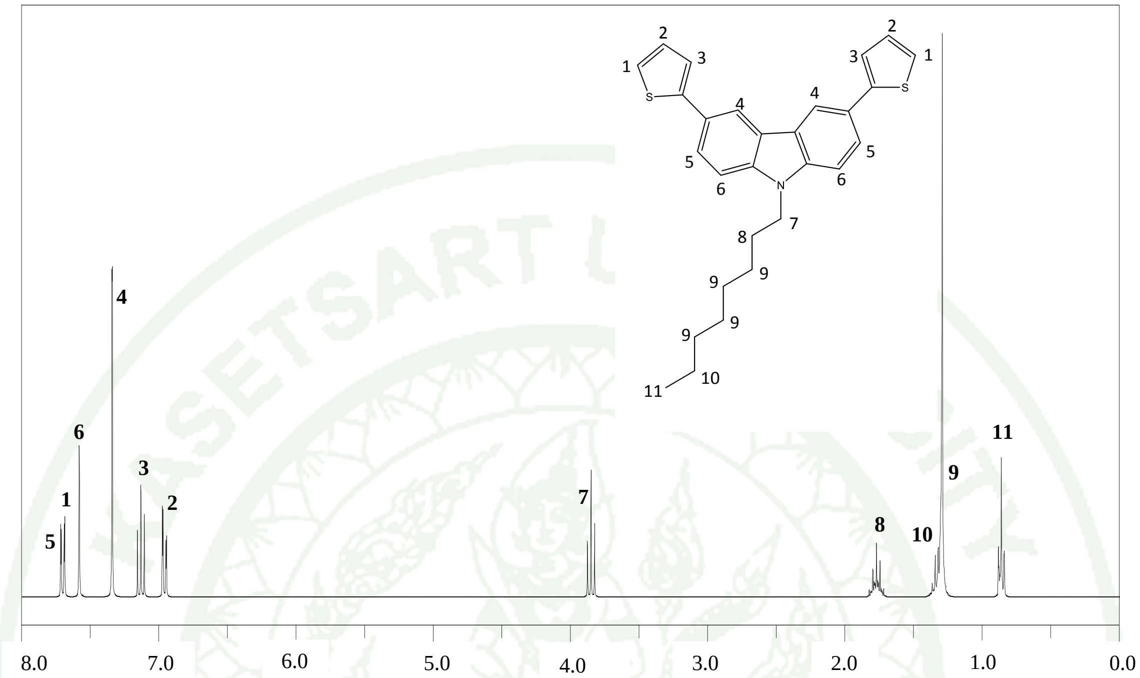

Appendix Figure A3 ^{1}H-NMR spectrum of 9-octyl-3,6-di(thiophen-2-yl)-carbazole.

4. 5,5’-(9-octyl-carbazole-3,6-diyl)-dithiophene-2-carbaldehyde

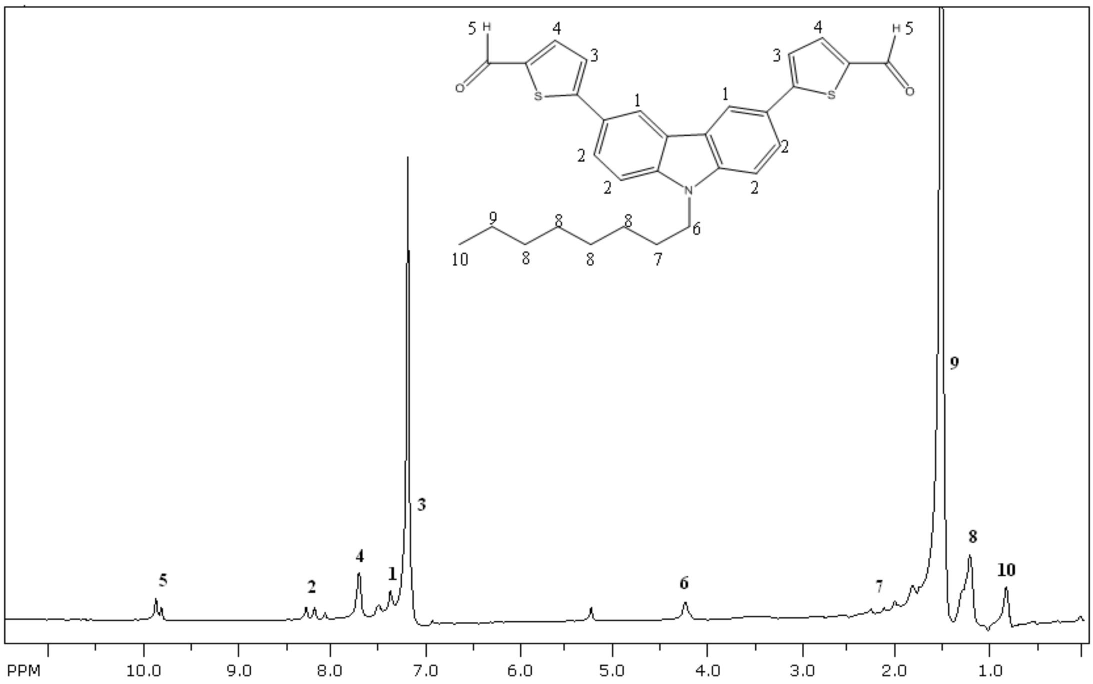

Appendix Figure A4 ^{1}H-NMR spectrum of 5,5’-(9-octyl-carbazole-3,6-diyl)-dithiophene-2-carbaldehyde.

5. 1,1’-(5,5’-(9-octyl-carbazole-3,6-diyl)-bis-(thiophene-5,2-diyl))-diethanone

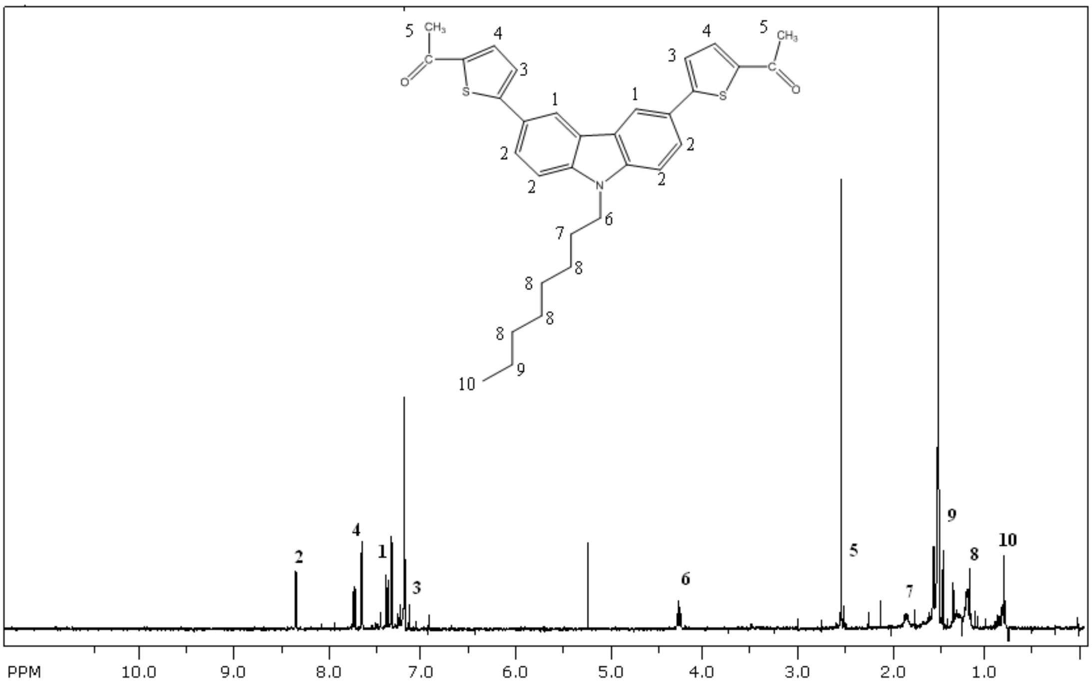

Appendix Figure A5 ^{1}H-NMR spectrum of 1,1’-(5,5’-(9-octyl-carbazole-3,6-diyl)-bis-(thiophene-5,2-diyl))-diethanone.

Radiative lifetime

The radiative lifetime of an excited electronic state in a laser gain medium is the lifetime which would be obtained if radiative decay via the unavoidable spontaneous emission were the only mechanism for depopulating this state. It is given by the equation

$$\frac{1}{\tau_{rad}} = \frac{8\pi n^2}{c^2} \int v^2 \, \sigma_{em}(v) dv = 8\pi n^2 c \int \frac{\sigma_{em}(\lambda)}{\lambda^4} d\lambda$$

which shows that high emission cross sections and a large emission bandwidth inevitably lead to a low radiative lifetime. This is because the cross sections describe not only the strength of stimulated emission but also that of spontaneous emission. The derivation of this equation is based on an equation for the mode density of free space as is also used e.g. for the derivation of Planck's law for the power spectral density of thermal radiation. This means that the equation does not hold in microcavities (as often used in experiments on quantum electrodynamics) because such cavities can substantially modify the mode density.

Note also the influence of the refractive index via the mode density. If fluorescence lifetime measurements are done using a powder with a grain size well below the wavelength of light, the refractive index of the ambient medium (rather than that of the powder grains) becomes relevant. For example, the upper-state lifetime measured for powder in air can be longer compared with that for solid crystals. Such observations should not be misinterpreted as evidence for quenching effects in crystals.

Another important aspect is that a shorter mean wavelength of the emission implies a shorter radiative lifetime. This results from the increased mode density of the radiation field. A consequence is that ultraviolet lasers tend to have a higher threshold pump power than e.g. infrared lasers.

As the gain efficiency of a laser medium is in simple cases proportional to the product of the maximum emission cross section and the upper-state lifetime (the $\sigma-\tau$ product), lasers based on broadband gain media have a higher threshold pump power. The actual lifetime of an electronic level can be lower than the radiative lifetime, if non-radiative quenching processes also significantly depopulate the level. This means that the quantum efficiency of the transition is below unity.

If the quantum efficiency is known to be close to unity, the above equation can be used for obtaining the absolute scaling of emission cross sections, the wavelength dependence of which is already known from the shape of the emission. In other cases, where the scaling of emission cross sections is known (e.g. obtained from absorption cross sections via the reciprocity method), the quantum efficiency of the fluorescence can be obtained by comparing the calculated radiative lifetime with the upper-state lifetime.

Appendix B

Presentation and proceeding

Proceedings

1. Suwannee Sriyab, Songwut Suremitr and Supa Hannongbua. **Theoretical Study on Structures and Electronic Properties of 9-octyl-3,6-di(thiophen-2-yl)-Carbazole Derivatives.** 15th International Annual Symposium on Computation Science and Engineering (ANSCSE15), Bangkok University, Bangkok, Thailand, 30 March-2 April 2011.

Theoretical Study on Structures and Electronic Properties of 9-octyl-3,6-di(thiophen-2-yl)-Carbazole Derivatives

S. Sriyab[1,2], **S. Suramitr**[1,2*], **and S. Hannongbua**[1,2]
[1]*Department of Chemistry, Faculty of Science, Kasetsart University, Bangkok 10900, Thailand*
[2]*Center of Nanotechnology KU, Kasetsart University, Bangkok 10900, Thailand.*
***E-mail**: fsciswsm@ku.ac.th; **Fax**: 02-562-5555 ext. 2176; **Tel.** 02-562-5555 ext. 2227

ABSTRACT

Molecular structural and electronic properties of 9-octyl-3,6-di(thiophen-2-yl)-Carbazole (Th-3,6-CZ) and its derivatives have been studied using density functional theory (DFT). Metyl (CH_3), formyl (CHO) and acetyl ($COCH_3$) substitutions have been applied on 9-octyl-3,6-di(thiophen-2-yl)-Carbazole to investigate the optical properties. All structures were optimized by M06-HF functional of calculations with the 6-31G(d) basis set. The electronic transition of structural geometries have been studied by PCM-TD-PBE0/6-311G(d,p) calculations based on ground state geometries at M06HF/6-31G(d) level. The obtained results indicate that calculated UV-vis absorption spectra of Th-3,6-CZ, CH_3-Th-3,6-CZ, $COCH_3$-Th-3,6-CZ and CHO-Th-3,6-CZ were found at 289, 296, 363 and 372 nm with respect to the experimental data of 302, 298, 365 and 393 nm, respectively. In additional, the polarizable continuum model was successfully applied to include solvent effect in the model which plays an important role on the absorption behavior.

Keywords: 9-octyl-3,6-di(thiophen-2-yl)-carbazole derivatives, Density functional theory, Absorption, Quantum chemical calculations.

1. INTRODUCTION

In 1987, the thin multilayer OLED was recognized as one of the potential technologies for the next generation of flat-panel display device. One of the simplest OLED is consisted of indium tin oxide (ITO) anode, hole-transporting layer (HTL), electron-transporting layer (ETL), and Mg-Ag cathode, in which HTL or/and ETL could act as the light-emitting layer [1,2]. The ITO anode is a transparent semiconductor, which was used for the hole injection due to its work function of 4-5 eV [3]. During last decade, the intensive research has been carried out to generate the material with high light emitting efficiencies [4], high thermal stability, and good amorphous film formation property [5]. The electro-luminescence (EL) characteristic of OLED materials depend on the appropriate HOMO and LUMO energy levels and the electron and hole motilities [6,7]. Much effort has been undertaken recently to develop flexible and tunable light-emitting diodes (LEDs) from conjugated polymers. Many conjugated polymers have been designed and synthesized to develop blue-, green-, and red-light-emitting materials [8]. They have some very interesting electronic and optical properties and have been investigated as advanced molecular electronic materials. 3,6-Substituted carbazoles have been proved to be effective charge transporting, electroluminescent and host materials with improved thermal and morphological stabilities [9]. The carbazole-based compounds demonstrate high thermal, morphological, chemical and environmental stability. Two basic properties of the fully aromatic carbazolyl group are the easy oxidizability of nitrogen atom and its ability to transport positive charge centers via the radical cation species. In this research, quantum chemical calculations are investigate on the structural, electronic and optical properties of 9-octyl-3,6-di(thiophen-2-yl)-carbazole derivatives by density functional theory method.

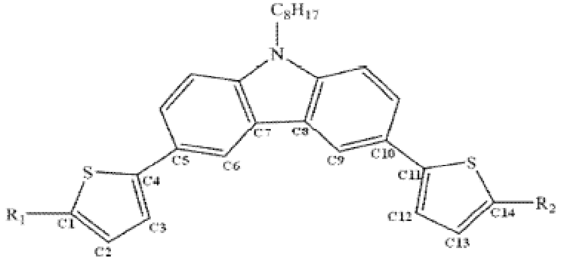

Figure 1. Structures of 9-octyl-3,6-di(thiophen-2-yl)-carbazole (R1=R2 = $-CH_3$, $-COCH_3$ and -CHO)

2. COMPUTATIONAL DETAILS

Starting geometries of 9-octyl-3,6-di(thiophen-2-yl)-carbazole derivatives (see in Figure 1), 9-octyl-3,6-di(thiophen-2-yl)-carbazole (Th-3,6-CZ), 1,1'-(5,5'-(9-octyl-carbazole-3,6-diyl)-bis-(thiophene-5,2-diyl))-diethanone (CHO-Th-3,6-CZ), 3,6-bis(5-methylthiophene-2-yl)-9-octyl-carbazole (CH_3-Th-3,6-CZ) and 5,5'-(9-octyl-carbazole-3,6-diyl)-dithiophene-2-carbaldehyde ($COCH_3$-Th-3,6-CZ) were constructed by Gaussian 03W package. For calculating the absorption and emission spectra, the geometry optimizations were performed by the density functional theory (TD-)DFT method with PBE0/6-31G(d) level of theory for the ground (S_0) and first singlet excited (S_1) states for all molecules. The electronic absorption and fluorescence spectra were computed by means of the TD-DFT (TD-PBE0/6-311G(d,p) method at the molecular structures optimized. The solvation effect on both the geometries and transition energies has been evaluated by means of the PCM approach. All calculations were performed using the Gaussian09 suite [10] of programs.

Table 1. Optimized bond lengths and torsion angle of R-3,6-CZ (R = H, CH_3, $COCH_3$ and CHO) obtained from M06HF/6-31G(d) and PCM-TD-PBE0/6-311G(d,p) methods

Paramerters	R=H		R=CH_3		R=$COCH_3$		R=CHO	
	S_0	S_1	S_0	S_1	S_0	S_1	S_0	S_1
Bond length (Å)								
C1-C2	1.376	1.371	1.378	1.374	1.378	1.394	1.380	1.395
C2-C3	1.421	1.413	1.422	1.412	1.409	1.393	1.407	1.392
C3-C4	1.375	1.395	1.373	1.385	1.383	1.404	1.385	1.404
C4-C5	1.465	1.459	1.464	1.448	1.462	1.432	1.461	1.432
C5-C6	1.409	1.421	1.409	1.421	1.400	1.427	1.400	1.427
C6-C7	1.392	1.403	1.392	1.403	1.391	1.373	1.390	1.373
C7-C8	1.444	1.436	1.444	1.425	1.444	1.459	1.444	1.459
C8-C9	1.392	1.402	1.392	1.403	1.391	1.373	1.390	1.373
C9-C10	1.409	1.421	1.409	1.421	1.400	1.427	1.400	1.426
C10-C11	1.465	1.459	1.464	1.447	1.462	1.432	1.461	1.432
C11-C12	1.375	1.395	1.393	1.385	1.383	1.404	1.385	1.404
C12-C13	1.421	1.413	1.422	1.412	1.409	1.393	1.407	1.392
C13-C14	1.376	1.371	1.378	1.375	1.378	1.394	1.380	1.395
Torsion angle (°)								
∠C3-C4-C5-C6	27.92	17.86	26.92	15.97	25.09	0.31	24.71	0.25
∠C9-C10-C11-C12	27.76	17.85	26.80	16.17	25.92	0.31	24.46	0.32

Table 2. PCM-TD-PBE0/6-311G(d,p)//M06HF/6-31G(d) in solvent phase

Electronic transitions	E_{ex} (eV)	E_{ex} (nm)	*f*	Wave function composition	Expt.
R=H					
Absorption					
$S_0 \rightarrow S_1$	3.61	342.76	0.0147	HOMO→LUMO (93%)	-
$S_0 \rightarrow S_2$	3.77	328.39	0.6536	HOMO→L+1 (94%)	-
$S_0 \rightarrow S_3$	4.16	297.96	0.6606	H-1→LUMO (88%)	302
$S_0 \rightarrow S_4$	4.24	292.01	0.1952	HOMO→L+2 (96%)	-
$S_0 \rightarrow S_5$	4.43	279.42	0.3487	H-1→L+1 (94%)	252
Fluorescence					
$S_1 \rightarrow S_0$	3.33	371.00	0.0184	HOMO→LUMO (95%)	-
$S_2 \rightarrow S_0$	3.55	348.78	0.6678	HOMO→L+1 (94%)	405
R=CH$_3$					
Absorption					
$S_0 \rightarrow S_1$	3.55	348.97	0.0133	HOMO→LUMO (94%)	-
$S_0 \rightarrow S_2$	3.71	334.16	0.8088	HOMO→L+1 (95%)	298
$S_0 \rightarrow S_3$	4.05	306.00	0.5525	H-1→LUMO (90%)	-
$S_0 \rightarrow S_4$	4.18	296.50	0.2510	HOMO→L+2 (97%)	-
$S_0 \rightarrow S_5$	4.33	285.97	0.3225	H-1→L+1 (96%)	-
Fluorescence					
$S_1 \rightarrow S_0$	3.26	380.00	0.0163	HOMO→LUMO (95%)	-
$S_2 \rightarrow S_0$	3.47	356.57	0.8277	HOMO→L+1 (95%)	356
R=COCH$_3$					
Absorption					
$S_0 \rightarrow S_1$	3.15	393.50	1.0077	HOMO→LUMO (97%)	365
$S_0 \rightarrow S_2$	3.44	359.62	0.2130	HOMO→L+1 (99%)	356
$S_0 \rightarrow S_3$	3.63	341.04	0.0022	HOMO→L+2 (61%)	-
$S_0 \rightarrow S_4$	3.81	324.76	0.2205	H-1→LUMO (64%)	-
$S_0 \rightarrow S_5$	3.84	322.57	0.2375	H-1→L+1 (68%)	318
Fluorescence					
$S_1 \rightarrow S_0$	2.79	444.06	1.2205	HOMO→LUMO (98%)	457
$S_2 \rightarrow S_0$	3.18	389.00	0.1935	HOMO→L+1 (98%)	-
R=CHO					
Absorption					
$S_0 \rightarrow S_1$	3.08	402.47	1.0083	HOMO→LUMO (97%)	393
$S_0 \rightarrow S_2$	3.38	366.45	0.1915	HOMO→L+1 (99%)	-
$S_0 \rightarrow S_3$	3.60	343.84	0.0306	H-1→LUMO (55%)	-
$S_0 \rightarrow S_4$	3.76	329.53	0.0934	H-5→LUMO (32%)	-
$S_0 \rightarrow S_5$	3.76	329.06	0.0187	H-4→LUMO (43%)	-
$S_0 \rightarrow S_6$	3.78	327.57	0.2242	H-1→L +1 (58%)	250
Fluorescence					
$S_1 \rightarrow S_0$	2.75	449.57	1.2196	HOMO→LUMO (98%)	475
$S_2 \rightarrow S_0$	3.15	393.22	0.1615	HOMO→L+1 (96%)	-

3. RESULTS AND DISCUSSION

The molecular structures of in the ground state (S_0) and the first singlet excited state (S_1) states were obtained by the (TD-)PBE0 method. The structure of Th-3,6-CZ, CH_3-Th-3,6-CZ, $COCH_3$-Th-3,6-CZ and CHO-Th-3,6-CZ were compared based on optimized geometries of the S_0 and the S_1 states given in Table 1. In Figure 1, the C-C bond lengths along the main chain were also compared based on the optimized geometries in the S_0 and S_1 states. The ground-state structures of all molecules are non-planar with the torsion angle ∠C3-C4-C5-C6 and ∠C9-C10-C11-C12 (about ~25°) because of the steric repulsion as in Table 1. The excitation to the S_1 state relaxes the bond alternation: the single bond lengths (C-C) were calculated to be contracted in the S_1 state and the double bond lengths (C=C) to be longer as shown in Table 1. The excited state-torsion angles are more planar than the ground state geometries.

For a better understanding of the electronic properties of molecules, the excitation energy was studied. The calculate absorption, fluorescence transition state of all molecules and the corresponding experimental values are presented in Table 2. The results show that the absorption spectra of Th-3,6-CZ, CH_3-Th-3,6-CZ, $COCH_3$-Th-3,6-CZ and CHO-Th-3,6-CZ is agreed well with the experimental spectra in dichloromethane solution. The PCM-TD-PBE0/6-311G(d,p) shows good agreement with the experiment. Absorption energies of of Th-3,6-CZ, CH_3-Th-3,6-CZ, $COCH_3$-Th-3,6-CZ and CHO-Th-3,6-CZ are 289, 296, 363 and 372 nm with respect to the experimental data of 302, 298, 365 and 393 nm, respectively. All of these states are assigned to the $\pi \rightarrow \pi^*$ transition corresponding to the transition from HOMO to LUMO, HOMO→L+1 and H-1→L+1 transitions. The introduction of $COCH_3$ and CHO groups on the 9-octyl-3,6-di(thiophen-2-yl)-Carbazole to bathochromic shift of the absorption wavelengths and fluorescence of carbazoles derivatives.

4. CONCLUSION

The structural and electronic properties of Th-3,6-CZ and derivatives were studied, based on quantum chemical calculations. The TD-PBE0/6-311G(d,p) method has been used for the physical properties of substituted model compound. Substitution on thiophene unit by various functional groups were considered and Th-3,6-CZ derivatives (Th-3,6-CZ, CH3-Th-3,6-CZ, COCH3-Th-3,6-CZ and CHO-Th-3,6-CZ). Most of the derivative of Th-3,6-CZ molecule exhibit planar structures at excitation state. The excited state-torsion angles are more planar than the ground state geometries. The obtained results of the electronic transition of structural geometries indicate that calculated UV-vis absorption spectra related with the experimental data.

REFERENCES

1. Tang, C. W., and Vanslyke, S. A., *Appl Phys Lett*, 1987, **51**(12), 913-915.
2. Fong Wallace, H. H., Choy, C. H., Hui, K. N., and Liang, Y. J., *Appl Phys Lett*, 2006, 8**1**(11).
3. Paliulis, O., Ostrauskaite, J., Gaidelis, V., Jankauskas, V., and Strohriegl, P., *Macromol Chem Phys*, 2003, **204**(14), 1706-1712.
4. Shirota, Y., Kuwabara, Y., Inada, H., Wakimoto, T., Nakada, H., Yonemoto, Y., Kawami, S., and Imai, K., *Appl Phys Lett*, 1994, **65**(7), 807-809.
5. Shirota, Y., Okumoto, K., and Inada, H., *Synthetic Met*, 2000, **111**, 387-391.
6. Pan, J. H., Chiu, H. L., and Wang, B. C., *J Mol Struc-THEOCHEM*, 2005, **725**(1-3), 89-95.
7. Brunner, K., Van Dijken, A., Börner, H., Bastiaansen, J. J. A. M., Kiggen, N. M. M., and Langeveld, B. M. W., *J Am Chem Soc*, 2004, **126**(19), 6035-6042.
8. Belletête, M., Bédard, M., Leclerc, M., and Durocher D., *J Mol Struc-THEOCHEM*, 2004, **679**(1-2), 9-15.

9. Yamashita, Y., Fujii, N., Murakata, C., Ashizawa, T., Okabe, M., and Nakano, H., *Biochemistry-US*, 1992, **31**(48), 12069-12075.
10. Frisch, M. J., Trucks, G. W., Schlegel, H. B., Scuseria, G. E., Robb, M. A., Cheeseman, J. R., Scalmani, G., Barone, V., Mennucci, B., Petersson, G. A., Nakatsuji, H., Caricato, M., Li, X., Hratchian, H. P., Izmaylov, A. F., Bloino, J., Zheng, G., Sonnenberg, J. L., Hada, M., Ehara, M., Toyota, K., Fukuda, R., Hasegawa, J., Ishida, M., Nakajima, T., Honda, Y., Kitao, O., Nakai, H., Vreven, T., Montgomery, Jr., J. A., Peralta, J. E., Ogliaro, F., Bearpark, M., Heyd, J. J., Brothers, E., Kudin, K. N., Staroverov, V. N., Kobayashi, R., Normand, J., Raghavachari, K., Rendell, A., Burant, J. C., Iyengar, S. S., Tomasi, J., Cossi, M., Rega, N., Millam, N. J., Klene, M., Knox, J. E., Cross, J. B., Bakken, V., Adamo, C., Jaramillo, J., Gomperts, R., Stratmann, R. E., Yazyev, O., Austin, A. J., Cammi, R., Pomelli, C., Ochterski, J. W., Martin, R. L., Morokuma, K., Zakrzewski, V. G., Voth, G. A., Salvador, P., Dannenberg, J. J., Dapprich, S., Daniels, A. D., Farkas, Ö., Foresman, J. B., Ortiz, J. V., Cioslowski, J., Fox, D. J. Gaussian 09, revision 02; Gaussian, Inc.: Wallingford, CT, 2009.

ACKNOWLEDGMENTS

This work has been supported in part by grants from the National Center of Excellence in Petroleum, Petrochemical Technology, Center of Nanotechnology Kasetsart University, Kasetsart University Research and Development Institute (KURDI), Laboratory of Computational and Applied Chemistry (LCAC), the Commission on Higher Education via the "National Research University Project of Thailand" (NRU).

CURRICULUM VITAE

NAME : Ms. Suwannee Sriyab

BIRTH DATE : May 8, 1986

BIRTH PLACE : Chiang Mai, Thailand

EDUCATION :

YEAR	INSTITUTE	DEGREE/DIPLOMA
2005-2009	Maejo University	B.Sc. (Chemistry)
2009-2011	Kasetsart University	M.S. (Chemistry)

POSITION/TITLE : Postgraduetes student

WORKPLACE : Faculty of Science, Kasetsart University

SCHOLASHIP : The Kasetsart University Research and Development Institute (KURDI), and National Nanotechnology Center (NANOTEC)

Postgraduate Education and Research Programs in Petroleum and Petrochemicals, and Advanced Materials (NCE-PPAM)

Kasetsart University Research and Development Institute (KURDI)